REVISTA ESPINHAÇO

Revista Espinhaço, 2025, 15 (1)

ISSN 2317-0611

The origin of diamond-bearing quartzite breccias from the Sopa Brumadinho Formation, Southern Espinhaço Range, Minas Gerais, Brazil

A origem das brechas quartzíticas diamantíferas da Formação Sopa Brumadinho, Serra do Espinhaço Meridional, Minas Gerais, Brasil

Pedro Angelo Almeida-Abreu
UFVJM
https://ORCID 0000-0001-6273-4809
pangelo.ufvjm@gmail.com

Renato Ferreira Miranda
LEV Brasil
renatogeoverdi@gmail.com

Gislaine Amorés Battilani
UFVJM
https://ORCID 0000-0003-2554-5253
gislaine.battilani@ict.ufvjm.edu.br

Eduardo Fontana
UFVJM
https://ORCID 0000-0002-1963-7795
eduardo.fontana@ict.ufvjm.edu.br

Abstract

The breccias of the Sopa-Brumadinho Formation, recognized as diamond-bearing since 1840, have had an igneous origin proposed since 1928. Their quartzite/metarenite clasts are millimetric to 50 cm, angular, pinkish to red in color, and similar to the substrate rocks. Their predominantly phyllitic matrix has a composition incompatible with that of igneous rocks, but REE data indicate a kimberlitic nature, *with* diamond xenocrysts, which can exceed 30 ct. The bodies (locally intrusive) have varying shapes—including a "champagne glass" shape—and reach up to 10 m thick and more than 50 m long. A proposed origin by cohesive debris flows from adjacent steep slopes appears unfeasible due to the consistent presence of diamonds in all deposits along a 50 km N–S extension. Since mudflows are not mineral concentrators and considering the absence of exotic material and the universal presence of diamonds, a proximal origin through the reworking of diamond-bearing tephra (tuff rings or pyroclastic surges) must be considered. Furthermore, the shape of the deposits and their contact relationships show that the breccias are confined within craters generated by phreatomagmatic volcanism, such as at Mina do Barro, where the breccias, circumscribed by quartzite walls, reach at least 60 m in depth. The physical characteristics of the gems reveal an absence of sedimentary reworking, and their mineral inclusions indicate a lithospheric origin for the diamonds. Regionally expressed lineaments appear to have acted as conduits for kimberlite magmas to reach the surface around ~1.7 Ga.

Keywords: Diamondiferous breccia; Sopa-Brumadinho Formation; phreatomagmatic volcanism; Southern Espinhaço range.

https://doi.org/10.5281/zenodo.17553543

Resumo
As brechas da Formação Sopa-Brumadinho, reconhecidas como diamantíferas em 1840, tem origem ígnea advogada desde 1928. Mostram clastos de quartzitos/metarenitos milimétricos a 50cm, angulosos, de coloração vermelha-rosada, semelhante às rochas do substrato. Sua matriz predominantemente filítica tem composição incompatível com rochas ígneas, mas as terras-raras mostram natureza kimberlítica e hospeda xenocristais de diamantes, que podem superar 30ct. Os corpos (localmente intrusivos), mostram formas variadas – inclusive em "taça-de-champagne" - e exibem espessuras de até 10m e extensão lateral maior que 50m. Uma suposta origem por fluxos de detritos coesivos oriundos de encostas íngremes mostra-se inviabilizada pela recorrência diamantífera em todos os depósitos numa extensão N-S de 50 km. E desde que *mudflows* não são concentradores de minerais e considerando a ausência de materiais exóticos e a presença universal de diamantes seria imperioso admitir origem proximal pelo retrabalhamento de tefra diamantífera (tu*ff-rings* ou *pyroclastic-surges*). Ademais, a forma de jazimento e relações de contato evidenciam que as brechas estão acondicionadas em crateras geradas por vulcanismo freatomagmático como na Mina-do-Barro, onde as brechas, circunscritas por paredes quartzíticas, alcançam pelo menos 60m de profundidade. As feições físicas das gemas revelam ausência de retrabalhamento sedimentar e suas inclusões minerais indicam origem litosférica dos diamantes. Lineamentos de expressão regional emergem como estruturas condutoras dos magmas kimberlítico à superfície em ~1.7 Ga.

Palavras-chave: Brecha diamantífera; Formação Sopa-Brumadinho; vulcanismo freatomagmático; Serra do Espinhaço Meridional.

1. **Introduction**

Diamond exploration in the Southern Espinhaço Range (SER) dates to the early 18th century, when the Diamond District was established, becoming the world's largest diamond producer until the mid-19th century. The region's diamonds were initially mined from alluvial and colluvial deposits of the drainage network (mainly the Jequitinhonha Basin) and, later (from the 19th century onward), also from conglomerates and breccias of the Sopa Brumadinho Formation (SBf). Although the rocks of the Espinhaço Supergroup exposed within the study area are metamorphosed and deformed, they almost always preserve their sedimentary identity and, therefore, will be referred to according to their respective protolith, without the use of the prefix meta- or metamorphic equivalents.

The source areas and primary rocks of diamonds have been the subject of controversy since the 19th century, based on two main hypotheses: (1) kimberlites from a source area outside the Espinhaço Basin, i.e., the São Francisco Craton; (2) syn-sedimentary volcanism associated with the SBf within the Espinhaço Basin. The quartzite breccias of the SBf, according to the autochthonous origin hypothesis, would represent vent breccias of phreatomagmatic magmatism from the final phase of SBf deposition (Almeida Abreu, 1996). On the other hand, from the perspective of diamonds originating outside the basin, the breccias would be sedimentary in origin, i.e., gravitational deposits of the debris flow type (Chaves, 1997; Uhlein, 1991), with diamonds derived from the interior of the São Francisco Craton and transported by the river system into the Espinhaço Basin.

https://doi.org/10.5281/zenodo.17553543

ISSN 2317-0611

Despite their economic importance and controversial origin, these breccias have received limited study regarding deposit geometry, petrography, and lithogeochemistry. Due to their friability and diamond content, most quartzite breccia deposits in the SER have already been almost completely mined, except for those in the João Boa and Córrego Novo mines, and the remaining deposits in the Barro Branco, Brumadinho, and Caldeirões mines. The Córrego Novo mine is currently the only one actively mining quartzite breccias in the SER.

In this work, therefore, the geological characterization of breccias from the Córrego Novo and Brumadinho mines was conducted through detailed geological mapping, stratigraphic section surveys, and lithogeochemical studies - integrated with investigations of mineral inclusions in diamonds from the region and the analysis of geophysical data (aeromagnetometry) provided by CODEMIG.

2. Geological Context

The Southern Espinhaço Range (SER), an orogenic belt that delimits the southeastern edge of the São Francisco Craton (Almeida, 1977) (Figure 1), extends northward from the Iron Quadrangle for approximately 300 km. It is predominantly composed of Paleo- to Mesoproterozoic rocks of the Espinhaço Supergroup (Almeida Abreu and Renger, 2002), especially metarenites/quartzites, pelites (phyllites), conglomerates, and volcanic rocks metamorphosed under greenschist facies conditions (Almeida Abreu, 1993; Dossin *et al*., 1984; Martins Neto, 1998, 2000; Schöll and Fogaça, 1979).

https://doi.org/10.5281/zenodo.17553543

REVISTA ESPINHAÇO
Revista Espinhaço, 2025, 15 (1)
ISSN 2317-0611

Figure 1. Simplified Geological Map of the Southern Espinhaço Mountain Range and adjacent regions (adapted from Renger *et al*., 2025).

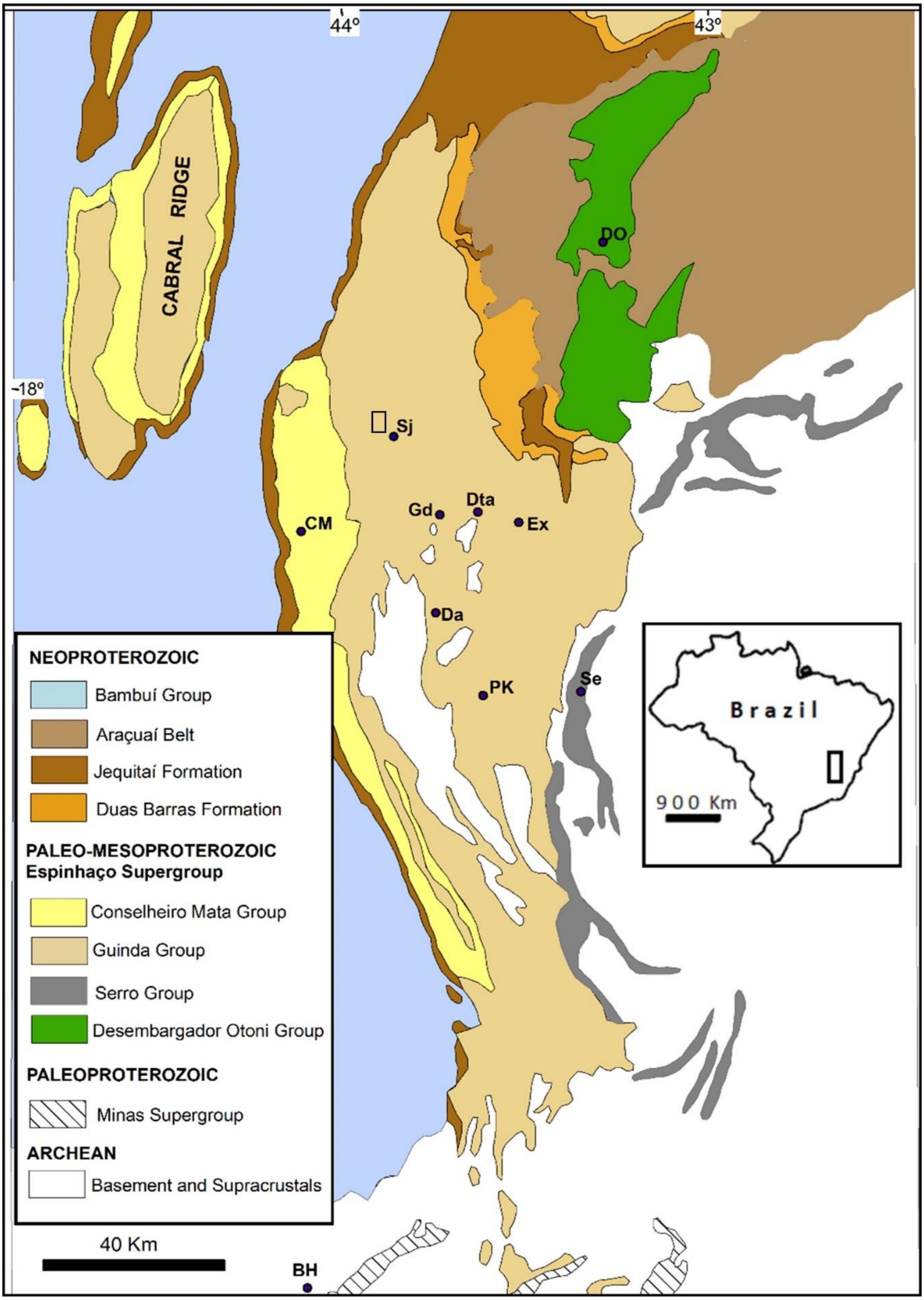

The rectangle locates figure 2. Towns and villages indicated on the map: CM – Conselheiro Mata; Da – Datas; DO – Desembargador Otoni; Dta – Diamantina; Ex – Extração; Gd – Guinda; PK – Presidente Kubitschek; Se – Serro; SJ – São João da Chapada.

https://doi.org/10.5281/zenodo.17553543

ISSN 2317-0611

The stratigraphic succession of the Espinhaço Supergroup was divided by Pflug (1968) into eight lithostratigraphic units. Pflug's column was revised in subsequent works and subjected to nomenclature adjustments (Pflug and Renger, 1973, Schöll and Fogaça, 1979), as well as subdivisions into smaller units and the grouping of formations into the Guinda (Knauer, 1990) and Conselheiro Mata (Dossin *et al*., 1984) groups. Sedimentological studies carried out since the 1980s have led to new interpretations of the depositional systems and the basinal context of the Espinhaço Supergroup units. (Garcia and Uhlein 1987; Dossin *et al*. 1984; Almeida-Abreu 1993; Uhlein *et al*. 1998; Martins-Neto 1998, 2000, Almeida-Abreu and Renger, 2007).

Figure 2. Geological map of the Córrego Novo mining area (original scale 1:8,000, Miranda, 2019).

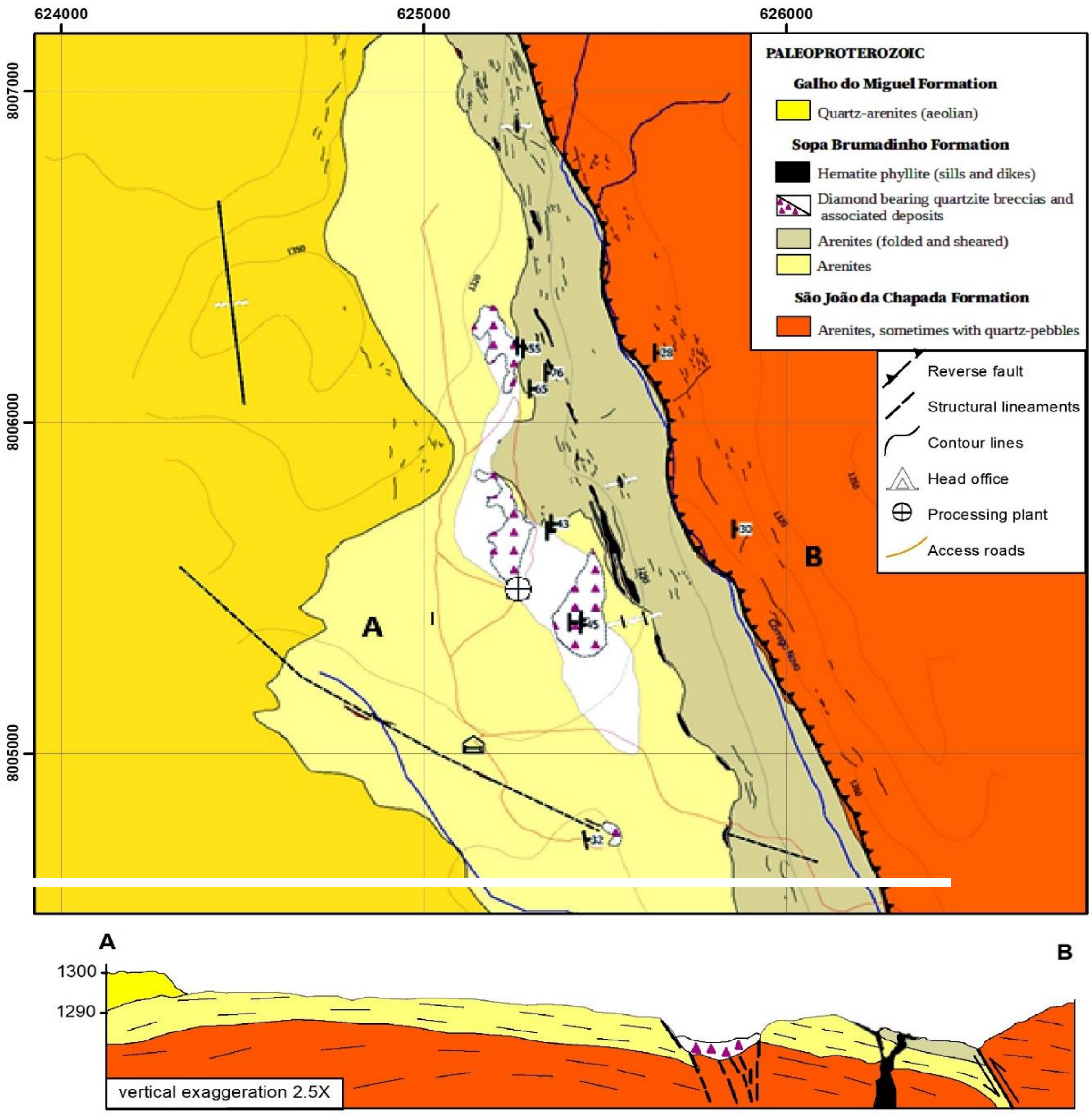

In section A-B, the structures observed under the site of the occurrence of quartzite breccias (subvertical black dashed lines) represent the conduits of phreatomagmatic injections.

https://doi.org/10.5281/zenodo.17553543

The SBf is of special relevance to this study, as it represents the only unit of the Espinhaço Supergroup mineralized in diamonds. It is composed essentially of siliciclastic sediments, including diamond-bearing conglomerates and, subordinately, basic and alkaline volcanic rocks, including vent breccias, i.e., the diamond-bearing quartzite breccias that make up the Campo Sampaio Member, the top unit of the SBf (Almeida Abreu, 1996). The Córrego Novo mine has quartzite breccias as the only rock mineralized in diamonds and is located in the diamond district of São João da Chapada – Campo Sampaio (Figure 2). Almeida Abreu and Renger (2007) presented the stratigraphic column of the successions that make up the Espinhaço System in the different domains of the SER, considering the respective basinal environments.

Martins-Neto (1998, 2000) proposed that the Espinhaço Basin would be a sag basin, assuming that the iron formations on the eastern edge of the SER would be of early Proterozoic age, belonging to the Minas Supergroup of the Quadrilátero Ferrífero. However, evidence of late Paleoproterozoic ages of these iron formations (Silveira-Braga *et al*., 2015; Rolim *et al*., 2016) reinforces the original model of Pflug (1965), i.e., the Espinhaço Basin configures a passive continental margin (originally defined as a geosyncline), and therefore, the iron formations were deposited on the continental shelf of the basin.

Other geological evolution models for the Espinhaço Supergroup deal with the occurrence of superimposed rifting at ~1700 Ma and ~1250 Ma, i.e., “sag cycles,” the latter remaining active during the Neoproterozoic until undergoing tectonic inversion in the Brasiliano Cycle (Chemale *et al*., 2012; Alkmim and Martins-Neto, 2012; Santos *et al*., 2013; Guadagnin and Chemale, 2015).

On the other hand, Almeida Abreu and Renger (2002, 2007) argue that the orogenesis of the SER occurred before 1 Ga, given that the glaciogenic deposits of the Macaúbas Group, which form fringes on the western and northeastern edge of the mountain range, are discordantly based on different units of the Espinhaço Supergroup. This glaciation ("Jequitaí Glaciation") occurred around 1 Ga (D’Agrella Filho *et al*., 1990), and this age is reinforced by the absence of clasts of basic rocks of the Pedro Lessa Suite (906 ± 2 Ma, Machado *et al*., 1989) in its glaciogenic deposits. This suite constitutes a LIP (Chaves *et al*., 2019) that currently occupies approximately 2.5% of the SER surface (Hoppe, 1986), and many of its dikes occupy 1st- and 2nd-order lineaments that cut tectonic structures shaped in rocks of the Espinhaço Supergroup.

Data and information on the evolution of geological knowledge of the Espinhaço Mountain Range, including different models of geological evolution, can be found in Renger (1979), Almeida Abreu (1993), and Renger and Knauer (1995). Discussions on the discovery,

https://doi.org/10.5281/zenodo.17553543

ISSN 2317-0611

exploration, and provenance of diamonds from the Espinhaço Mountain Range were presented by Chaves *et al*. (1998, 1999), Almeida Abreu and Renger (1999, 2001), and Renger *et al*. (2025).

3. Material and methods

The work was developed in different stages. In the pre-field stage, the lineaments marked by anomalies in the magnetometric images (CODEMIG, 2001, scales 1:80,000 and 1:30,000) were traced and classified into three groups based on the intersection relationships between them. The representation of morphostructural lineaments was performed on Google Earth satellite images at a scale of 1:30,000, while shaded relief maps (illumination direction of 315° and inclination of 45°) were generated from SRTM images provided by USGS Earth Explorer. By superimposing the lineament maps on the detailed geological map of the Córrego Novo Mine area, we sought to establish correlations between the lineaments and structures with the regional distribution of quartzite breccias. During the pre-field phases a bibliographic survey was also carried out, accompanied by a synthesis of regional geology with a special focus on the bibliography dealing with the geology of diamond districts. Furthermore, bibliographic research was carried out on diamond geology, as per the summary provided in the chapter of this article.

The subsequent stage was dedicated to the survey of detailed geological sections in the Córrego Novo and Brumadinho mines, accompanied by the description of 64 outcrops and the collection of 26 rock samples. Of the collected samples, nine (three hematitic phyllites and six diamondiferous quartzite breccias) were selected for petrographic studies from thin sections prepared in the rock lamination laboratory of CeGeo and described in a Zeiss Axio-LabA1 petrographic microscope of the Microscopy Laboratory of CeGeo/UFVJM. The mineral phases not recognized by the microscope were analyzed in a scanning electron microscope (SEM), using a HITACHI TM 3000 equipment with EDS attached from the multiuser laboratory of UFVJM.

Two samples of reddish phyllites, two samples of kaolinized phyllites from two decimetric dikes embedded in quartzites of the bedrock under breccia body and two samples of quartzite breccia matrix were selected for lithogeochemical studies, analyzed by the SGS - GEOSOL Laboratory to obtain the content of major and minor elements using ICP-OES (inductively coupled plasma optical emission spectrometry) and trace elements (Ba, Sr, Zn, Zr, V, Co, Cs, Cu, Ga, Hf, Mo, Nb, Ni, Rb, Sn, Ta, Tb, Th, Tl, U, W, Y) and rare earths using ICP-MS (inductively coupled plasma mass spectrometry).

https://doi.org/10.5281/zenodo.17553543

ISSN 2317-0611

Additional gravimetric studies were performed using a Sintrex CG-05 gravimeter, provided by the National Observatory within the PegBR program. Data acquisition was obtained through three 30-second readings, with four profiles being executed in the Córrego Novo mine area, with an approximate spacing of 30 meters between points. The data were processed using the GTraj software and interpolated using the minimum curvature technique, resulting in the Bouguer anomaly map (Figure 3).

4. The Córrego Novo Mining (MCN)

4.1. Location

The MCN is located in an elevated area that is part of the plateau (altitudes slightly above 1400 asl) of the São João da Chapada – Campo Sampaio Diamond District. In this district, diamond mining in rocks has always been carried out in quartzite breccias of the SBf, that is, in the mines of Barro, Pagão, Campo Sampaio Velho and Novo, Água Fria, João Boa and Córrego Novo. The MCN occupies the elevated western flank of the Córrego Novo (a 1st order tributary of the right bank of the upper Rio Pardo Grande) approximately 10 km to the NW of São João da Chapada, which is approximately 30 km from Diamantina. The location of the mining front where part of the sections and sampling were carried out has the coordinates UTM – WGS84 – 23K – 625266m E; 8006242m S.

Mineral exploration at MCN, then as semi-mechanized mining, has its first records of activity in the early 1970s. However, it was referred to by Thompson (1928) and Correns (1932) as a locus of "faiscagem" (rudimentary method of manual mining) since the first quarter of the 20th century). From 2015 onwards, it was taken over by Córrego Novo Mining with the mechanized exploitation of quartzite breccias and, in places, colluvial deposits in the vicinity of the mine pits. The open pits are implemented in the area where quartzite breccias occur and the dismantling operation is carried out with hydraulic jets and backhoes, with the material being transported by trucks to the pre-concentration site where, under aqueous flow, the clayey material is separated from the denser residues, and these are transported to the jigs of the concentration plant. MCN management information reports production of 3,131.84 ct between 2017 and 2024, an average of 448.27 ct/year, generally 3/1 diamonds (i.e., 3 diamonds to add up to 1 ct). The largest diamonds extracted from the Córrego Novo Mine were 6.30; 7.85; 8.27; 9.30; 11.45; and 33.48 ct, the latter extracted in December 2022.

4.2. Summary of the Geology of the MCN Area

ISSN 2317-0611

The three formations that make up the Guinda Group outcrop in the MCN area (Figure 2). The lower unit, the São João da Chapada Formation, occupies the eastern part of the map, dominating the eastern flank of the Córrego Novo. It features rugged relief with predominantly exposed bare rock interspersed with restricted areas of shallow, sandy soil. It consists exclusively of fine- to medium-grained sandstones, locally coarse, occasionally with the presence of sparse, subangular to rounded granules or pebbles of milky quartz. Plane-parallel lamination is defined in decimetric to metric beds and banks, and tabular cross-stratifications with thicknesses of 40 cm to over one meter are common and sometimes abundant. Contact with the overlying unit does not outcrop in the map domain and its lower contact is marked by an inverse fault that juxtaposes it with rocks of the SBf throughout its western limit (Figure 2). The occurrence of hematitic phyllites along the margin of this fault throughout its extension (Figures 2 and 3) and considering the synsedimentary origin of these phyllites, suggests that this is a past normal fault, reactivated during the tectonic inversion. This fault, in addition, is conjugated to the first-order crustal lineaments (Figure 8).

The SBf occupies the entire central part of the map, forming a NNW-SSE direction band with a width of 350 to 1000 meters. The SBf is limited to the east by a semi-linear reverse fault (N20W) that juxtaposes the São João da Chapada Formation along the entire length of the contact between these two formations and whose lineament hosts the Córrego Novo thalweg. To the W, the SBf is concordantly covered by quartz-arenites of the Galho do Miguel Formation. The SBf, within the scope of the MCN, shows a predominance of fine to coarse-grained sandstones, moderately selected, highlighting beds in centimetric to decimetric layers, in places defining metric-scale banks. Cross-stratifications are abundant, predominantly of the trough type with high width/height ratios, although tubular and tangential types are also frequent, whose dimensions vary from decimetric to metric and with paleocurrents indicating flow in the dominant W to E direction. The maturity of the sediments, their sedimentary structures and directional flow of the paleocurrents suggest that they are fluvial deposits of a braided channel system.

The eastern strip of the SBf exposure area, i.e., the strip adjacent to the reverse fault that juxtaposes the São da Chapada Formation (Figure 2), exhibits particular tectonic deformation, i.e., a ductile-brittle deformation zone marked by conspicuous foliation (S_1) trending N5 to 15W and dipping to the ENE (45-55°), highlighted mainly in hematitic phyllites rocks. Tight anticlines of submetric to metric order are molded in quartzites of this zone, occasionally associated with reverse faults of centimetric to metric rejects displacement seen on their W-vergent ramps.

https://doi.org/10.5281/zenodo.17553543

ISSN 2317-0611

The hematitic phyllite dikes are embedded (locally intercalated) in the quartzites with thicknesses that can reach up to 12 meters and, apparently, compose a swarm of dikes parallel to the preferred shear direction (NNW-SSE) (see section of Figure 2). The hematitic phyllites outcropping in the MCN area are similar to those described by Knauer and Schrank (1993) and Bezerra Neto (2016), that is, they exhibit medium to dark gray coloration and mineral composition of sericite, hematite and iron oxides, which may appear as nodules or defining millimeter bands. The mottled texture that stands out in some places may reflect the original texture of the protolith. Petrographic analysis shows the predominance of sericite (65-70%) and iron oxides (30-35%) and as accessories tourmaline (1 to 3%) and quartz (~1%). Sericite composes a very fine matrix, sometimes showing completely sericitized tabular whitish spots, which may represent pseudomorphs of feldspars. Iron oxides occur dispersed throughout the rock associated with tourmaline and quartz crystals. They also show a banded texture due to the alternation of iron oxides and sericite with millimetric to centimetric thicknesses. Associated with the hematitic phyllites is another rock of igneous character, that is, reddish phyllites with a red-colored clayey matrix, sometimes with pseudomorphs of small tabular crystals, interpreted as fully sericitized feldspars. These rocks are invariably highly altered, making them difficult to recognize in the field. In old pit sections in the northern part of the area, a small outcrop of these rocks associated with quartzite breccias stands out.

The abundance of hematitic phyllites in this more deformed band and considering that they are paleo-laterites/-bauxites from alteration of igneous rocks (Knauer and Schrank, 1993) reveals the synsedimentary tectonic activity of the fault that accommodates the Córrego Novo thalweg. On the other hand, the deformation related to the SER orogenesis is marked by conspicuous schistosity superimposed on the hematitic phyllites and the associated tight folds, as well as by quartz veins (occasionally smoky quartz composing well-formed crystals) of centimetric to decimetric thicknesses that fill joints of different orientations. In some mining fronts, quartz veins also appear embedded in sandstones and quartzite breccias.

https://doi.org/10.5281/zenodo.17553543

ISSN 2317-0611

Figure 3. Gravimetric map of the Córrego Novo Mine area.

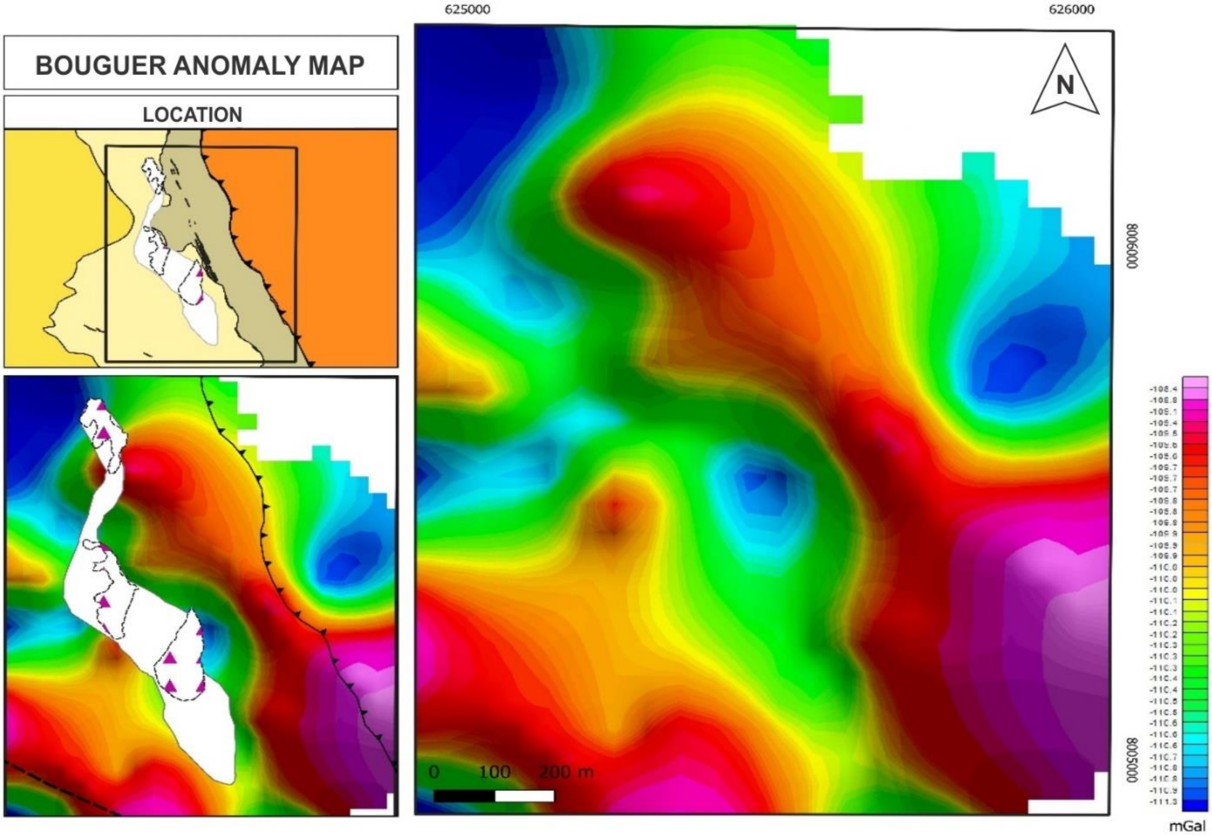

It can be seen that the largest NNW-trending anomaly is aligned with the various hematitic phyllite bodies (see the insert in the upper left corner and compare with Figure 2). The breccia bodies are aligned in the same direction (bottom left corner insert) but displaced to the W in relation to the anomaly. The WNW-ESE-trending anomaly appears to be related to the basaltic rock of the Pedro Lessa Suite.

The expression of the hematitic phyllite bodies (or of a large subsurface body that would have fed the different dikes shown in Figure 2) is expressed in the Bouguer anomaly map (values from -111.3 to -108.4 mGal), obtained by performing gravity profiles in the MCN area (Figure 3). The positive gravity anomaly aligned in the N30°W direction coincides with the fault line and with the outcrops of hematitic phyllites and reddish phyllites, therefore, an anomaly related to the high content of iron minerals.

The sandstones of the Galho do Miguel Formation occupy the entire western portion of the MCN area (Figure 2), with rugged relief and elevations that can project more than 200 meters relative to adjacent areas. Plane-parallel lamination is the predominant sedimentary structure, defining centimetric to metric beds and layers. In some places, the presence of tangential cross-stratifications of metric thickness is common, sometimes forming aeolian dunes with a height of more than 8 meters and lateral extension tens of meters. Petrographically, they are fine-grained quartz-arenites with some sericite and iron oxides. Occasionally, the rounding (spherical) of the quartz grains is preserved, characterizing the aeolian nature of the sediments. The Galho do Miguel Formation concordantly covers the SBf successions that include the

https://doi.org/10.5281/zenodo.17553543

ISSN 2317-0611

diamondiferous breccias (Figure 2) and is therefore a stratigraphic reference to indicate that these breccias are positioned in the upper part of the SBf.

4.3. Quartzite breccias from Córrego Novo and Brumadinho mines

The quartzite breccias from the MCN are invariably mineralized in diamonds, composing bodies of metric to decametric thicknesses (up to 25 meters) and of variable lateral extensions (Figure 4), that is, on the order of a few to many tens of meters (50 to 120 meters). Without regular spacing, the breccia bodies occur aligned in the NNW direction for at least 1 km (Figure 2), thus appearing parallel to the Córrego Novo fault. The breccias commonly appear as irregular and shapeless bodies inserted in pelitic and/or arenitic rocks of the same formation, defining lenses of varying dimensions (Figure 4a), but occasionally they form "champagne glass" shapes. The contacts of the breccias with the sandstones and/or phyllites are abrupt and show varied configurations, from tabular contacts, apparently concordant, to quite irregular contacts (Figure 4a, e), including surfaces strongly inclined in relation to the bedding. They are matrix-supported with a large predominance of angular to subangular clasts (rarely subrounded) of pink to reddish sandstones with dimensions ranging from millimeters to over 40 cm, immersed in a greenish pelitic matrix, often kaolinized, when it acquires a whitish coloration (Figure 4b). Rounded to subangular milky quartz clasts (sometimes with saccharoidal texture) are rare. Sandstone clasts often exhibit primary lamination or banding (Figure 4b), as well as granulometric variations and rarely centimeter-sized cross-stratifications. The uniform coloration, i.e., without zoning, indicates that this oxidation is pre- or syn-sedimentary, being contemporary or prior to the incorporation of clasts for the formation of the breccia, especially because it is observed (e.g., in the Brumadinho and Barro Branco mines) white clasts arranged next to red clasts. The occasional occurrence of clasts with millimetric fractures filled with pelitic (kaolinized) material suggests the action of fluid pressure in the brecciation process and formation of the rock (Figure 4c).

In the mining front in July/2019, in the northern vicinity of the beneficiation plant (UTM 625154 - 8005603), the exposed quartzite breccias were over 5 meters thick and covered by a package of altered pelites (phyllites – Fig. 4d), highlighting plane-parallel stratifications defined by millimetric to centimetric alternation denoted by variations in the color of the pelitic levels (greenish x whitish x grayish). The predominance of pelites in aggradational arrangement suggests lacustrine deposition within a small maar-type crater.

Subvertical dikes embedded in the pelites, or sandstones are rare (Almeida Abreu and Renger, 2001), but they didactically highlight the intrusive nature of the diamond-bearing

https://doi.org/10.5281/zenodo.17553543

ISSN 2317-0611

quartzite breccias of the SBf (Figure 4f). In the quartzite bedrock, beneath the breccia bodies, it is common to see dozens of greenish phyllite dikes (often kaolinized) with millimeter to centimeter thickness, in vertical to subvertical positions. They generally trend from N-S to NW-SE, sometimes NE (Figure 5b), and run through the rocky substrate beneath the breccia bodies (Figures 5a and b). Swarms of these small phyllite dikes provide evidence, in some places, of the fragmentation process of the host rocks promoted by phreatomagmatic volcanism (Figure 5c).

https://doi.org/10.5281/zenodo.17553543

ISSN 2317-0611

Figure 4. (a) Thick bodies of quartzite breccia in the MCN pit. They appear to be amalgamated bodies related to successive phreatomagmatic intrusions. Note the abrupt and irregular contact of the breccia with the host arenites. (b) Detail of the breccia highlighting clasts measuring millimeters to more than 15 cm immersed in a conspicuously foliated pelitic matrix. (c) Clasts exhibiting narrow millimeter-sized fractures filled with pelitic (kaolinized) material. (d) Section approximately 7 meters high showing a succession of stratified pelites covering the breccias in the mining pit front in July/2019. The predominance of pelites in aggradational arrangement suggests lacustrine deposition within a small maar-type crater. (e) Detail of discordant contact of the breccia on substrate arenites. (f) Intrusive body of quartzite breccia (approximately 50 cm thick) embedded in arenites, exposed in an old MCN pit (UTM 655188 – 800633

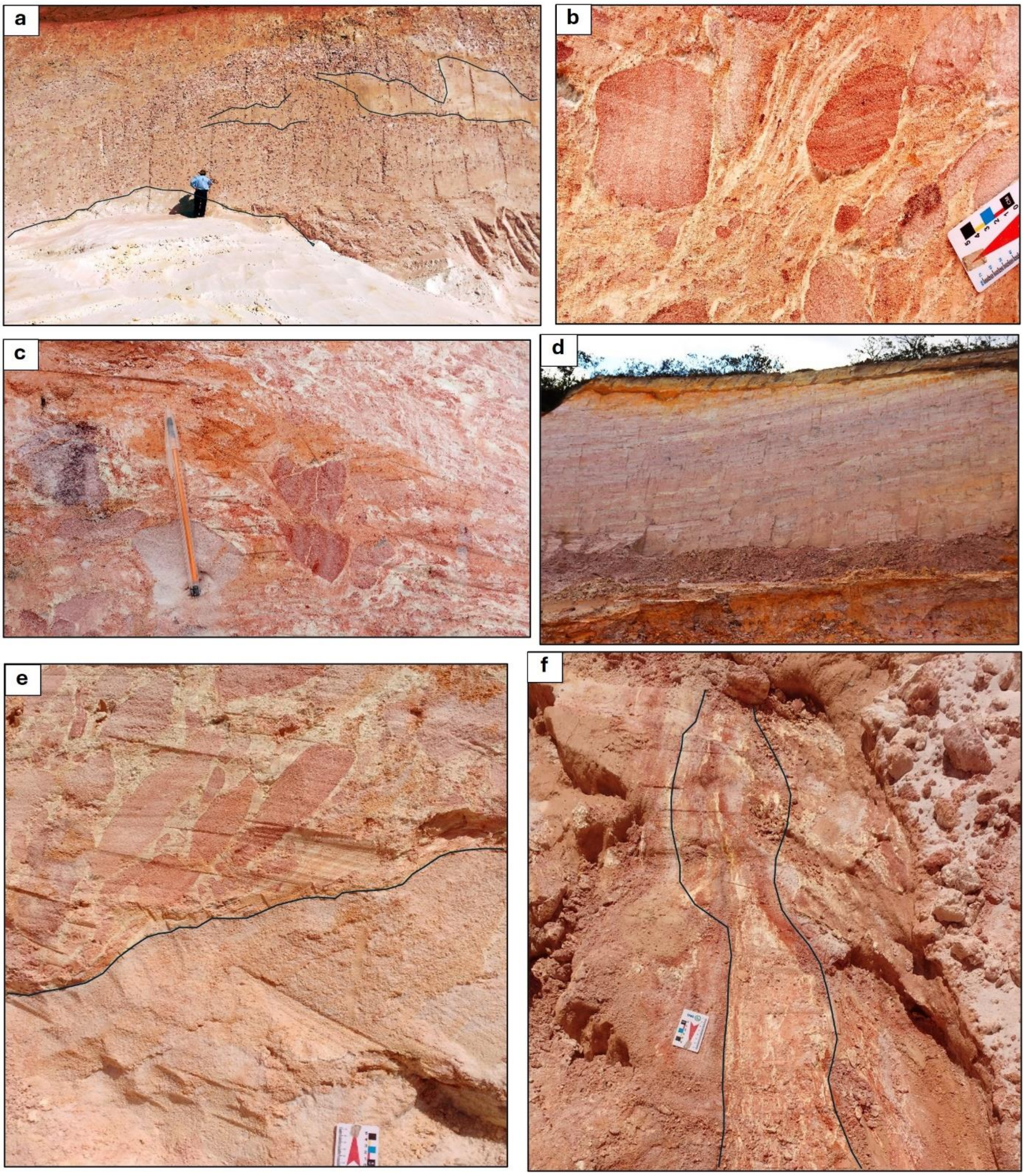

https://doi.org/10.5281/zenodo.17553543

ISSN 2317-0611

Figure 5. (a) Intrusive breccia body in arenites (MCN pit April/2024 - UTM 625548 8005265). The breccia exposed in the whitish subvertical section in the background cuts through layers of red sandstones at the contact on the left end of the photo. In the foreground, the reddish sandstones of the bedrock stand out, and above them the breccia body forms a semi-arc, denoting visibly discordant contacts. The hammer indicates the position of Photo b. (b) Kaolinized phyllite dike (5-6 cm thick) embedded in the bedrock arenites, projecting towards the contact of the breccia with the sandstones. It forms a bundle of NE-SW trending dikes. (c) Multiple mm-cm phyllite (kaolinized) dikes embedded in red bedrock arenites, evidencing the fragmentation process of the host rocks promoted by phreatomagmatic volcanism.

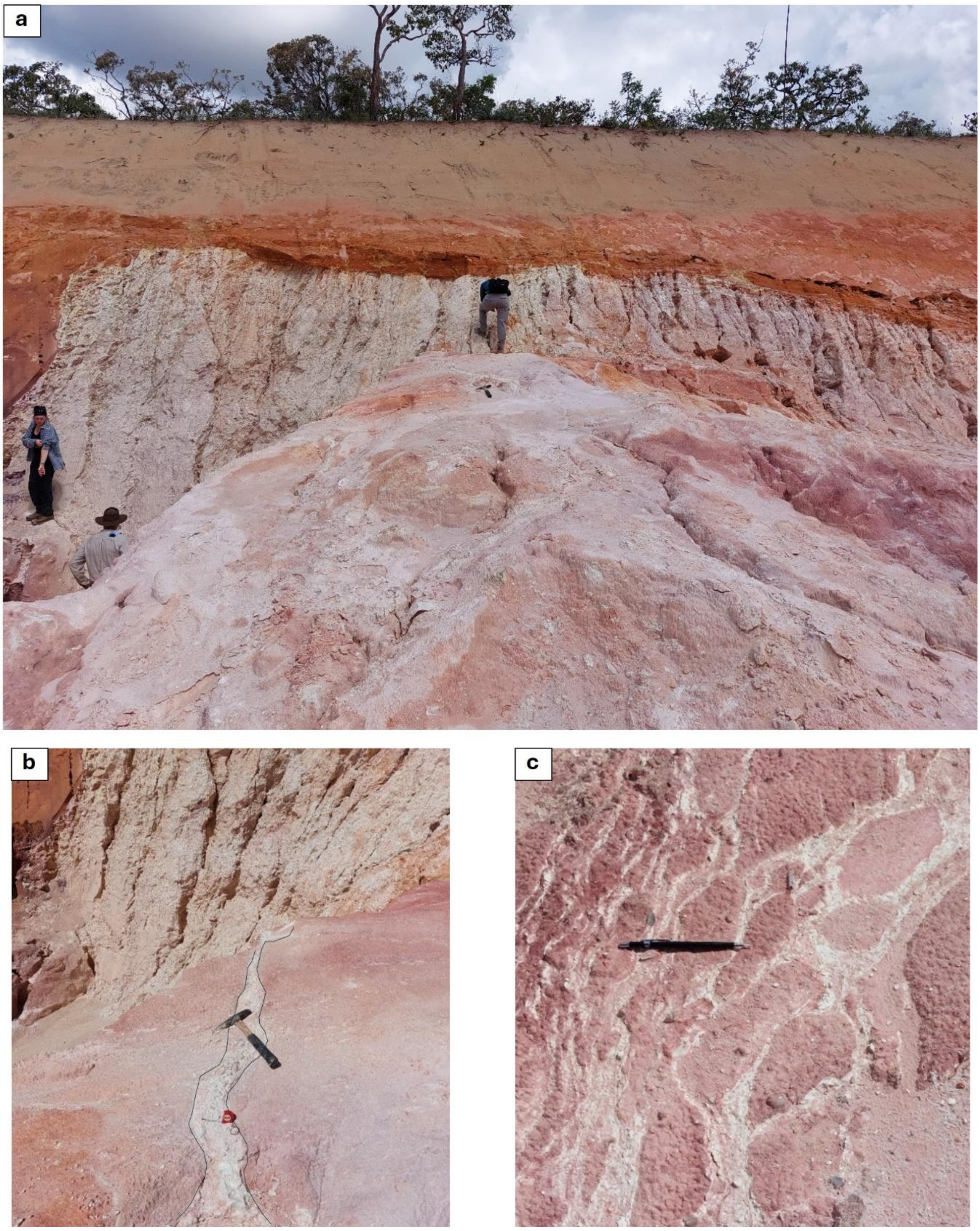

A petrographic study of the breccia matrix was performed after impregnation with resin to produce thin sections. Under the microscope, extensive presence of quartzite lithic fragments and quartz grains (50-55%) immersed in the sericitic matrix (40-45%) is observed, with frequent presence of opaque minerals (iron oxides), titanium oxides (according to SEM–EDS analyses, probably titanomagnetite and rutile, up to 2%) and rare zircons (<1%) (Figure 6a). The quartz grains are angular to subrounded, generally with undulatory extinction, frequently fractured and exhibiting corrosion at the edges (Figure 6b). Sericitized euhedral grains appear to represent "ghosts" of feldspars or feldspathoids (Figure 6c).

Quartzite breccias from other mines, both in the São João da Chapada-Campo Sampaio and in the Sopa-Guinda districts, show similar characteristics, i.e., angular quartzite clasts, generally reddish in color, predominantly pelitic matrix and invariably containing diamonds. Quartzite breccias occur invariably in the upper part of the SBf, always associated with a succession of pelites containing layers of sandstone and siltstone, as seen in sections from the Brumadinho Mine (Guinda District - Figure 7).

5. Structural Lineaments

The analysis and interpretation of aeromagnetometric images enabled the identification of structural lineaments revealed by the magnetic intensity signals. Three main groups of lineaments were recognized, which were active in different tectonic events. In the cratonic domains the largest lineaments stand out, which can be referred to as 1st order structures. However, these and other lower order lineaments (in terms of linear extension of the segments and not the number of segments) generally have recurrent movements as a result of tectonic cycles and events that have involved the cratons since Archean times. The analysis of the lineaments imprinted in cratonic areas covered by sedimentary successions and/or orogenic belts almost always show records of synsedimentary activities related to extensional tectonics, as well as to the subsequent reactivations promoted by the Precambrian orogenic cycles (Figure 8).

The recognized lineaments present, according to their orientations, different dimensions and frequencies, in addition to showing age relationships between them. Quantitatively, the WNW-ESE trending lineaments are predominant, especially in the northern half of the SER and Serra do Cabral (Figure 8a,b), and, although segmented, the segments are often perfectly aligned for extensions of many tens of kilometers. Chaves (2013), considering that these lineaments are filled by rocks from the Januária mafic dike swarm of Mesoproterozoic age, related them to the intracratonic rifting responsible for the formation of the Espinhaço Superior basin.

https://doi.org/10.5281/zenodo.17553543

ISSN 2317-0611

The second most abundant lineaments are the NE-SW trending lineaments, which generally preserve extensions slightly larger than the WNW-ESE pattern. However, the lineaments with the largest extension (although infrequent) exhibit NNW-SSE orientation, standing out as the youngest family (and, or of late reactivations), since they overlap the others (Figure 8b). Their first-order character is marked by significant extension and continuity in intermittent segments, and they commonly intercept all lineaments of other directions, therefore, of more recent kinematic activity. Its preferred northwest direction (N20-30°W) inflects to N40°W in the São Francisco Craton domain (Figure 8a) from where it extends continuously in an *echelon* pattern for more than 350 km, entering the SER through its NW domain, and being marked by strong positive magnetic anomalies.

The longest of these NNW-SSE trending lineaments, maintaining its *en echelon* pattern, traverses the São João da Chapada - Campo Sampaio diamond district, continuing to the Sopa-Guinda diamond district and then to the São Gonçalo do Rio das Pedras region, until it intersects the SER in its central-eastern domain (Figure 8a). Along its course, the lineament crosses the diamond-bearing districts at a distance of less than 10 km from their respective mines. Caldas *et al*. (2019) interpret that this lineament constitutes a large reactivated normal fault and that it would have acted in the opening of the Espinhaço Basin and, associated with smaller structural lineaments, would have been responsible for the compartmentalization of the basin.

https://doi.org/10.5281/zenodo.17553543

ISSN 2317-0611

Figure 6. Photomicrographs of MCN breccia matrix (images on the left side under natural light and those on the right side under crossed Nicols).

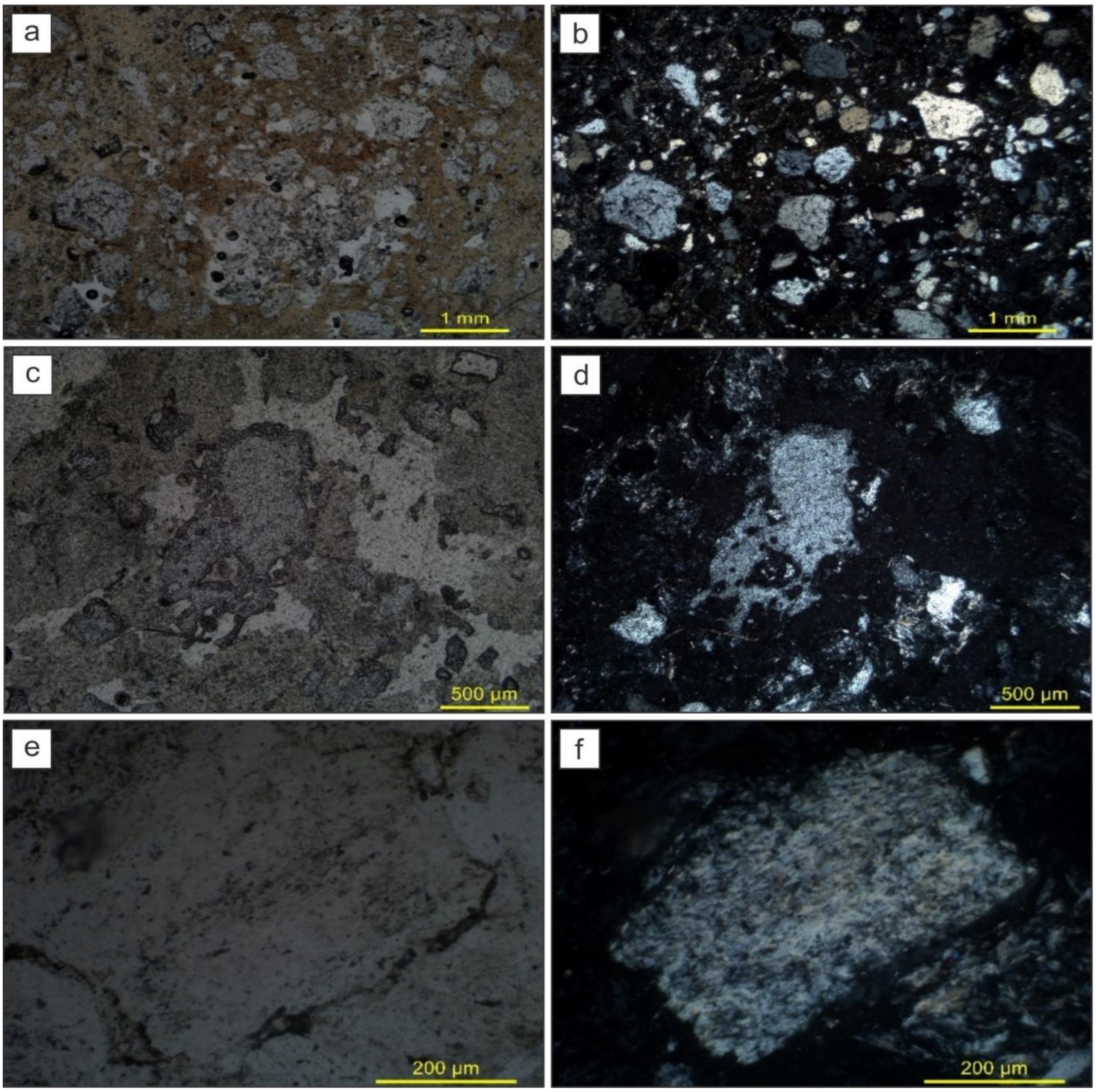

(a) and (b) The breccia matrix shows quartzite and quartz grains, and opaque minerals embedded in a sericitic (partially kaolinized) matrix. (c) and (d) Matrix image of the breccia showing intensely corroded quartz grains. (e) and (f) Image of breccia matrix showing sericitized rectangular euhedral grain, which may represent a feldspar or feldspathoid "ghost".

This proposal of Caldas *et al*. (2019) is not supported by observations in the rocks of the São João da Chapada and Sopa Brumadinho formations, given that the paleocurrent record of fluvial sediments from these formations invariably shows a W-to-E sedimentary flow. The quasi-unidirectional sedimentary flow was obviously determined by the paleo-relief and N-S synsedimentary faults that controlled the direction and propagation of the basin, which is consistent with the general orientation of the Espinhaço basin. The basin's compartmentalization was modulated primarily by W-E or WNW-ESE trending transfer faults (Almeida Abreu, 1995).

Figure 7. Section in the south-central segment of the Brumadinho Mine.

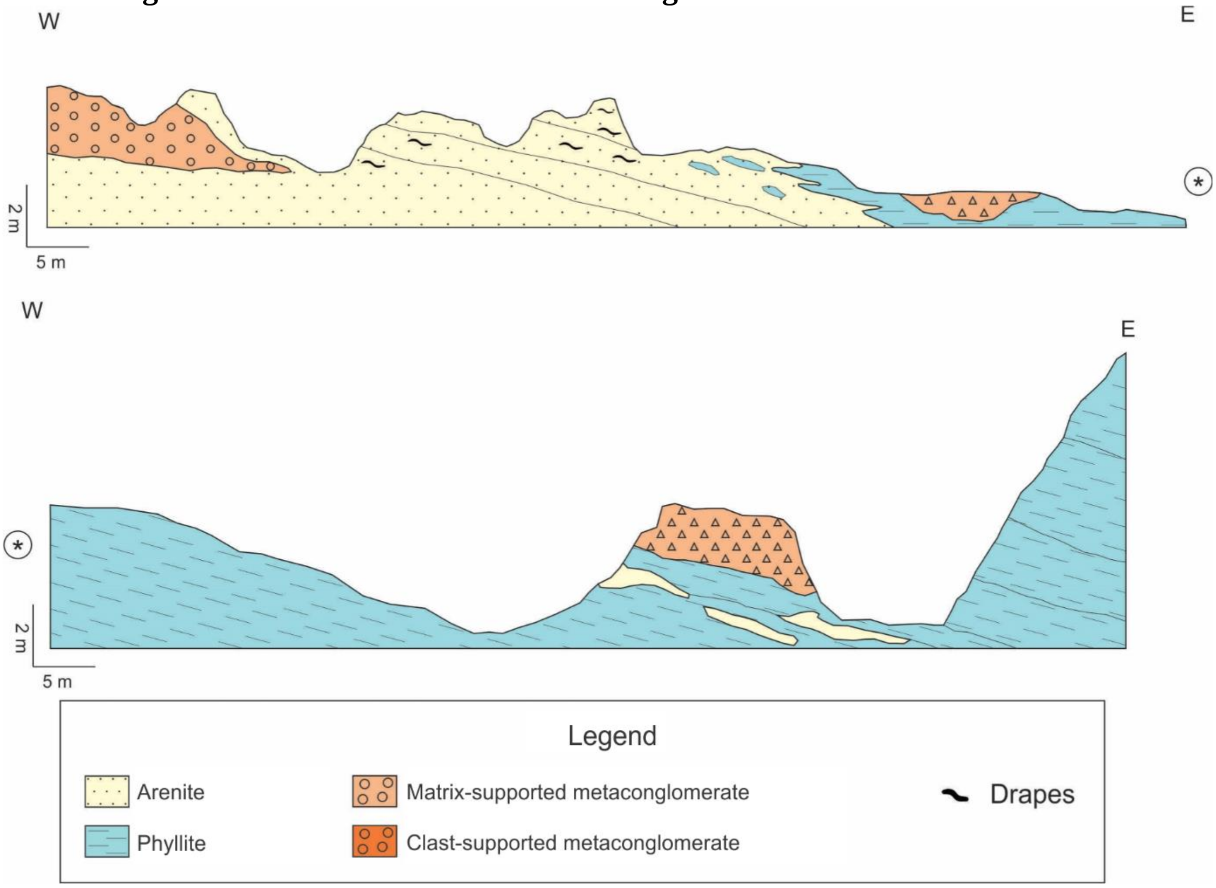

Note the different geometry of the breccia bodies and their association with pelitic rocks. A few dozen meters to the east of the upper-eastern part of the section, sandstones of the Galho do Miguel Formation outcrop overlying the SBf pelites, demonstrating that the breccias are included in the upper part of the lithostratigraphic unit. UTM location at the ends of the section: WNW Point (639612 – 7882795) and ESE Point (639767 – 7982729).

Furthermore, a pair of lineaments that are part of this NNW-SSE family individualize the SER of the northern segment of the orogenic belt, i.e., the northern Serra do Espinhaço (Figure 8a, b). These lineaments can be interpreted as dextral strike-slip faults that would have been responsible, therefore, for the segmentation of the Serra do Espinhaço before the end of its orogenesis, since the termination of both segments is covered by fringes of glaciogenic rocks from the Jequitaí Glaciation (~1. Ga, D´Agrella Filho *et al*., 1990).

The lineaments with the largest population within the SER, that is, those with a WNW-ESE direction, are revealed by a notable magnetic anomaly, as they are almost always filled with basic rocks of the Pedro Lessa Suite. Almeida-Abreu (1993, 1995) admits that these lineaments were very active during the crustal extension of the Espinhaço Basin, effectively influencing the paleogeographic arrangement of the basin.

The major lineaments in the domains outside the SER, that is, those with a NW-SE orientation, are also filled with basaltic rocks which, dated by the Ar-Ar method (Chaves and Neves, 2005), revealed a crystallization age of 135.72 +/- 4 Ma. According to Chaves (2003), these mafic dikes are part of the Transminas dike swarm, and their formation is associated with intracontinental rifting related to the opening of the South Atlantic.

The lineaments with a preferential northeast direction (N10-30° E) are mostly marked by positive magnetic anomalies and a bundle of these lineaments are prominent in the diamond district of São João da Chapada, also being present in the diamond districts of Sopa-Guinda, Extração, Datas and Presidente Kubitschek. According to Chaves (2013), these are associated with the Formiga lineaments (900-100 Ma) and are also commonly filled by the Pedro Lessa Suite dike swarm.

The satellite and SRTM images present morphostructural lineaments and highlight all the lineaments identified in the aeromagnetometric anomaly images (Figure 8d, e), also evidencing the greater frequency of lineaments with WNW-ESE directions.

It is possible to observe that, in the diamond district of São João da Chapada, the magnetic lineaments with NE-SW and WNW-ESE orientation intersect very close to the diamond mines, especially in the MCN area. The mine area is marked by a significant morphostructural lineament with an approximate NNW direction, which intersects the NE-SW and WNW-ESE magnetic lineaments (Figure 8c).

6. Lithogeochemistry

The chemical composition of the matrix of quartzite breccias (M-B), phyllite dikes (D) and reddish phyllites (FV) from the Córrego Novo mine can be seen in Table 1. The matrix of quartzite breccias exhibits high levels of SiO_2 (64 - 75%) and Al_2O_3 (15 - 24%) and low to moderate levels of K_2O (2 - 3%), Fe_2O_3 (1%), MgO (0.6 - 1%), TiO_2 (0.4 - 0.7%) and, to a lesser extent, CaO (0.02%), Na_2O (0.03%) and P_2O_5 (0.05%). However, the influence of their clasts and the host quartzite rocks on the composition of the matrix is evidenced by the pervasive contamination of quartz, also observed in thin sections of the rock (Figure 6 a, b).

Furthermore, the sediments and rocks of the continental successions of the Espinhaço Supergroup were subjected to severe weathering during and after sedimentation, which promoted leaching and profound alteration of the rocks and sediments especially in the rocks and sediments that contained labile minerals (Almeida Abreu, 1993). These conditions of severe weathering are also indicated by the absence of clasts from the basement and diamond source rock (including their satellite minerals) in the conglomerates and breccias of the SBf. On the

https://doi.org/10.5281/zenodo.17553543

other hand, the hematitic phyllites are records of the hot and humid climate during the deposition of the São João da Chapada and Sopa Brumadinho formations, as they are recognized as paleo-laterite/-bauxite deposits from the weathering alteration of volcanic rocks (Knauer and Schrank, 1993). The current exposure of the SBf successions (probably since the Pleistocene, Amaral-Santos *et al*. 2019) represents another weathering cycle imposed on the rocks of the unit, which contributes to the restrictions on the geochemical characterization (especially in relation to the major elements) of all rocks of igneous origin.

With regard to minor elements and rare earths, indications of the nature of the rocks, that is, of the reddish phyllites, the matrix of the breccias and the synsedimentary “phyllite” dikes (Table 1) are seen when comparing the samples with diagrams of the primitive mantle (Figure 9). It can be seen that the quartzite breccias, “phyllite” dikes and reddish phyllites have very similar behavior in the negative anomalies of Sr, Nb and Ti and positive anomalies of Th, K and Zr.

https://doi.org/10.5281/zenodo.17553543

ISSN 2317-0611

Figure 8. (a) and (b) Structural lineaments of the SER (outlined by the strong black line) recognized by anomalies from aeromagnetometric surveys, and from SRTM (morphostructural) and satellite images. The black points S, G, and E in image (b) locate the villages of Sopa, Guinda and Extração, respectively. (c), (d) and (e) Detail of the structural lineaments in the diamond district of São João da Chapada – Campo Sampaio, including the MCN area (identified by the crossed hammers). 1 - João Boa Mine; 2 - Campo Sampaio Mine; 3 - Água Fria Mine; 4 - Pagão Mine; 5 - Barro Mine.

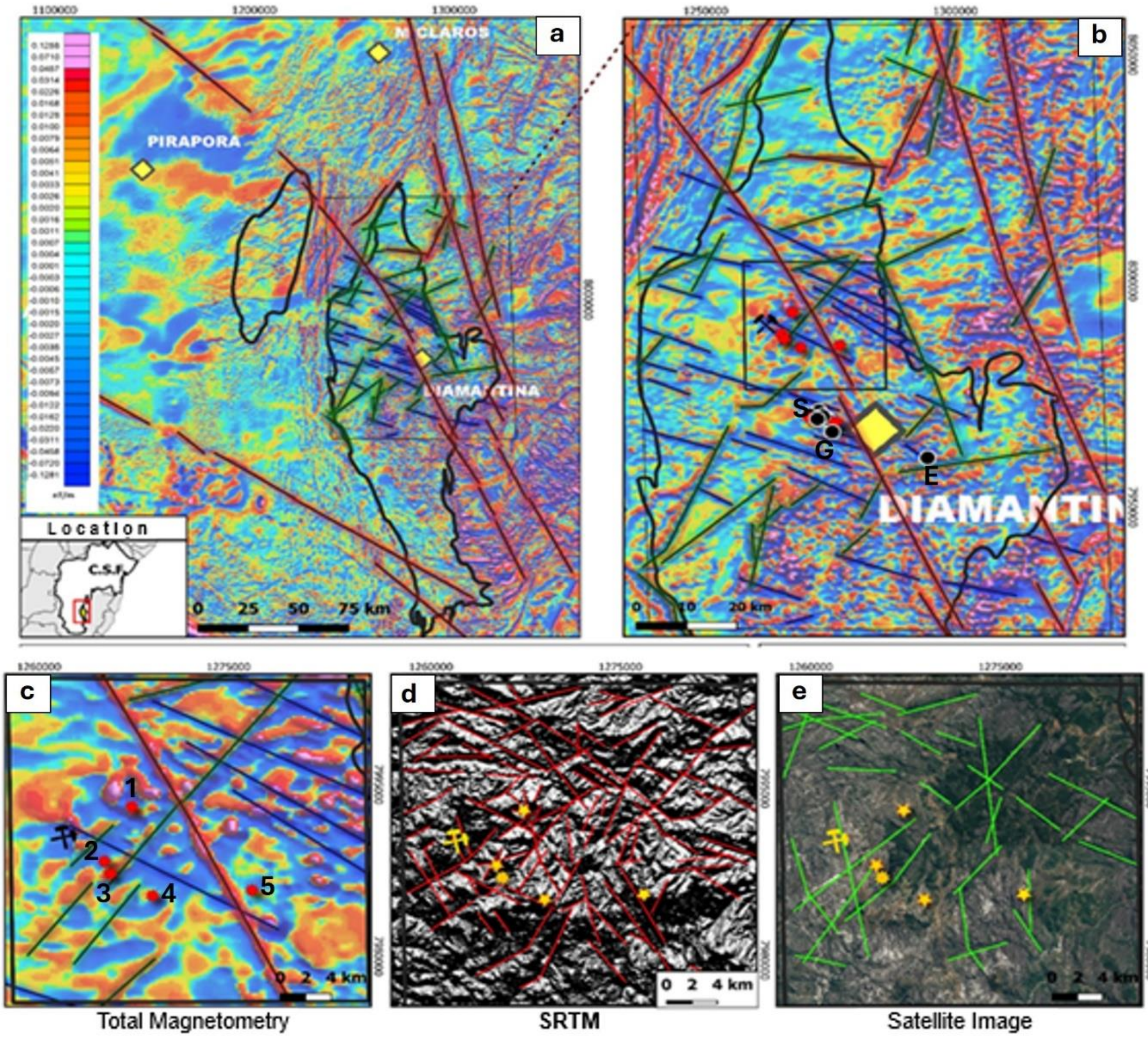

The total rare earth elements of the breccias are enriched by 10 to 200 times more than those of the chondrites. The distribution curve indicates a preferential fractionation of light rare earths with ratios of La/Yb ranging from 13 to 28 with an average of 20.51, while the negative anomaly of Europium (Eu/Eu*) is 0.18 - 0.2.

https://doi.org/10.5281/zenodo.17553543

REVISTA ESPINHAÇO

Revista Espinhaço, 2025, 15 (1)

ISSN 2317-0611

Table 1. Chemical composition of the matrix of diamond breccias (M-B1, MB-2), phyllite dikes (D1, D2) and reddish phyllites (F-A1, F-A2) of MCN. Major elements expressed as weight percentage and trace elements and rare earths in ppm.

	M-B1	M-B2	D1	D2	F-A1	F-A2
SiO_2	64,77	75,88	63,75	50,59	45,11	45,04
Al_2O_3	24,65	15,68	22,19	29,55	35,04	35,63
CaO	0,02	<0,01	0,03	0,04	<0,01	<0,01
Cr_2O_3	<0,01	<0,01	<0,01	<0,01	0,02	0,01
Fe_2O_3	1,59	1,0	1,86	3,05	5,5	4,8
K_2O	2,09	3,25	3,16	5,28	0,57	0,62
MgO	0,57	0,97	0,88	1,51	0,15	0,16
MnO	<0,01	<0,01	<0,01	<0,01	<0,01	<0,01
Na_2O	0,03	0,02	0,03	0,07	0,01	0,02
P_2O_5	0,05	0,04	0,01	0,03	0,11	0,13
TiO_2	0,73	0,39	0,53	0,83	1,2	1,02
LOI	8,1	3,98	6,53	8,27	13,32	13,31
Ba			273	527		
Sr	13	<10	<10	28	<10	<10
Zn	23	19	<5	8	101	80
Zr	392	507	552	660	1166	1229
V	121	24	<5	36	146	28
Co	1,1	0,9	1,3	2,3	11,1	10,2
Cs	0,48	0,41	0,81	1,67	0,09	0,08
Cu	12	6	11	11	37	26
Ga	21,8	13,1	18	29,6	32,7	28,6
Hf	8,49	11,69	12,16	15,1	30,4	30,09
Mo	3	<2	<2	<2	3	<2
Nb	12,86	6,36	10,55	18,21	20,98	18,99
Ni	12	9	9	15	211	184
Rb	35,6	39,6	59,2	104	7,1	7,5
Sn	2,5	1	5,3	6,7	2,1	1,7
Ta	0,71	0,43	0,51	1,36	1,92	1,77
Tb	0,35	0,35	0,74	0,94	1,36	162
Th	25,7	10,9	28	28,1	33	30,5
Tl	<0,5	<0,5	<0,5	<0,5	<0,5	<0,5
U	1,82	2,4	2,65	2,59	5,09	4,26
W	1,9	2,1	1,8	5,4	1,9	0,8
Y	12,79	14,67	51,32	30,72	47,62	47,96
La	53,5	26,5	22,7	53,4	36,7	45,2
Ce	117,8	42,4	60,1	110,5	91,2	116,6
Pr	9,95	4,66	3,44	8,37	6,06	9,66
Nd	32,1	16,8	11,7	27,3	28,3	42,2
Sm	3,7	2,6	2,2	6,5	7,1	9,7
Eu	0,62	0,47	0,58	1,56	1,71	2,33
Gd	2,47	2,42	3,55	6,65	8,66	11,82
Tb	0,35	0,35	0,74	0,94	1,36	1,62
Dy	2,02	2,14	6,82	5,85	8,4	8,54
Ho	0,42	0,48	1,56	1,13	1,75	1,73
Er	1,45	1,68	5,75	3,76	5,4	5,04
Tm	0,25	0,26	0,86	0,55	0,85	0,84
Yt	1,9	2	6,1	4	6,2	6
Lu	0,32	0,28	0,93	0,54	0,96	0,9

https://doi.org/10.5281/zenodo.17553543

ISSN 2317-0611

Figure 9. Representation of the analyzed samples in the primitive mantle composition diagram of Sun and McDonough (1989) and of the REE in the chondrite diagram of Anders and Grevesse (1989). MB – diamond bearing quartzite breccias; FV - reddish phyllites.

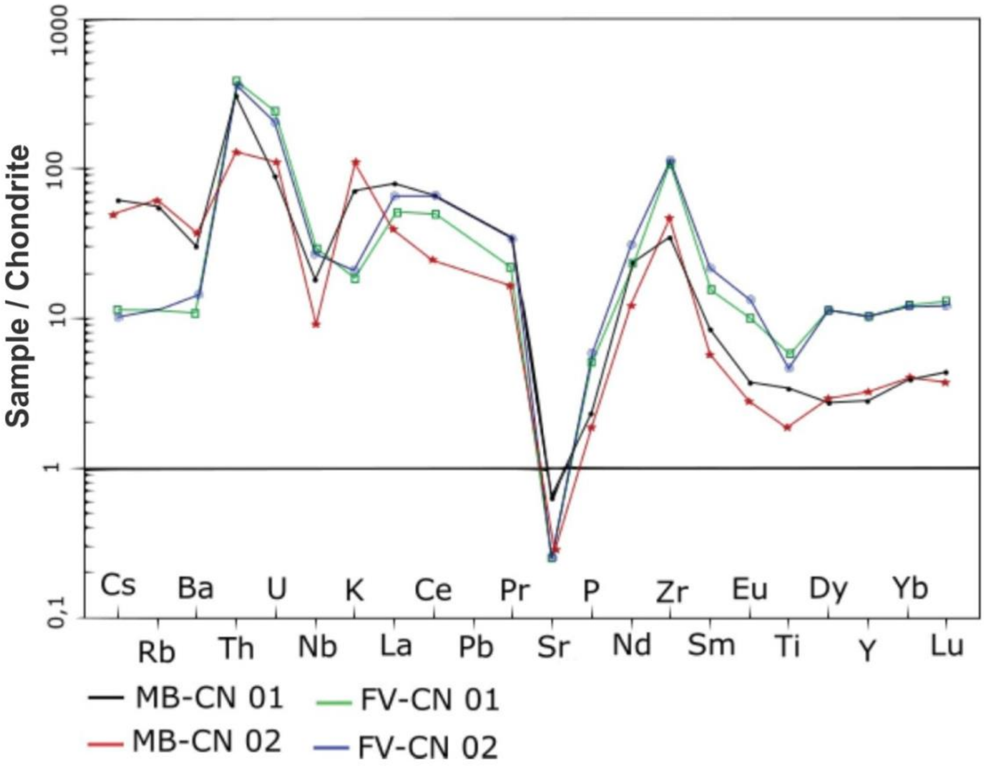

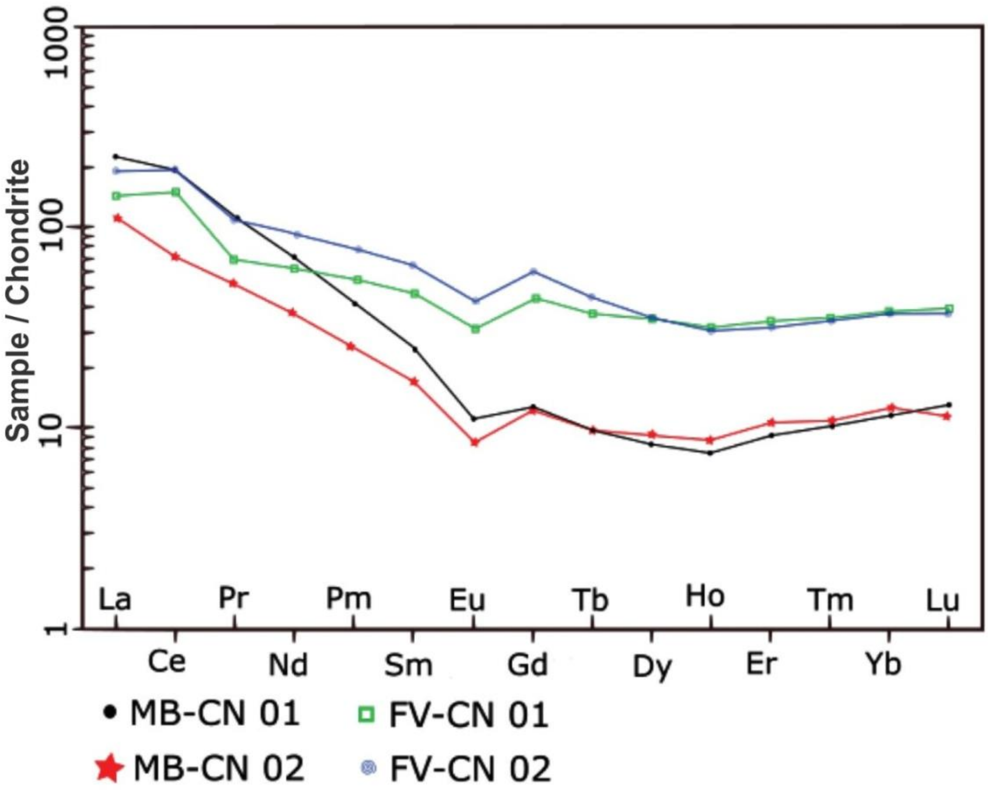

https://doi.org/10.5281/zenodo.17553543

ISSN 2317-0611

The reddish phyllites are basic rocks composed essentially of SiO_2 (45%), Al_2O_3 (35%), Fe_2O_3 (4.8-5.5%) and subordinately TiO_2 (1-1.2%), K_2O (0.5-0.6%), MgO (0.15%). The total rare earth elements of these reddish phyllites are enriched by 60 to 200 times more than those of the chondrites, and the distribution curve indicates a slight preferential fractionation of the light rare earths, with ratios of La/Yb ranging from 5 to 7, and the negative anomaly of Europium (Eu/Eu*) is 0.21.

The REE patterns of the breccias and reddish phyllites show a strong correlation of 0.808 using the Pearson correlation coefficient. In relation to the reddish phyllites, the breccias present a similar LREE pattern and are more depleted in HREE. Comparing the fractionation ratio of the REE using the La/Yb ratio, it is possible to verify that the breccias present a much higher average pattern (20.51) than the reddish phyllites (6.48).

Figure 10 – Comparison of the REE patterns of breccias (MB), reddish phyllites (FV), and phyllite hematitic (average patterns of the Bezerra Neto, 2016; and Cabral *et al.* 2012); olivine lamproites (Jacques *et al.*, 1989); phlogopite lamproites (Mitchell and Bergman, 1991), and micaceous kimberlites (Mitchell and Brunfelt, 1975). Note that the breccias present a negative gap relative to the REE of hematitic phyllites and reddish phyllites but present a LREE fractionation similar to that of hematitic phyllites, with the correlation index between breccias and hematitic phyllites being 0.95.

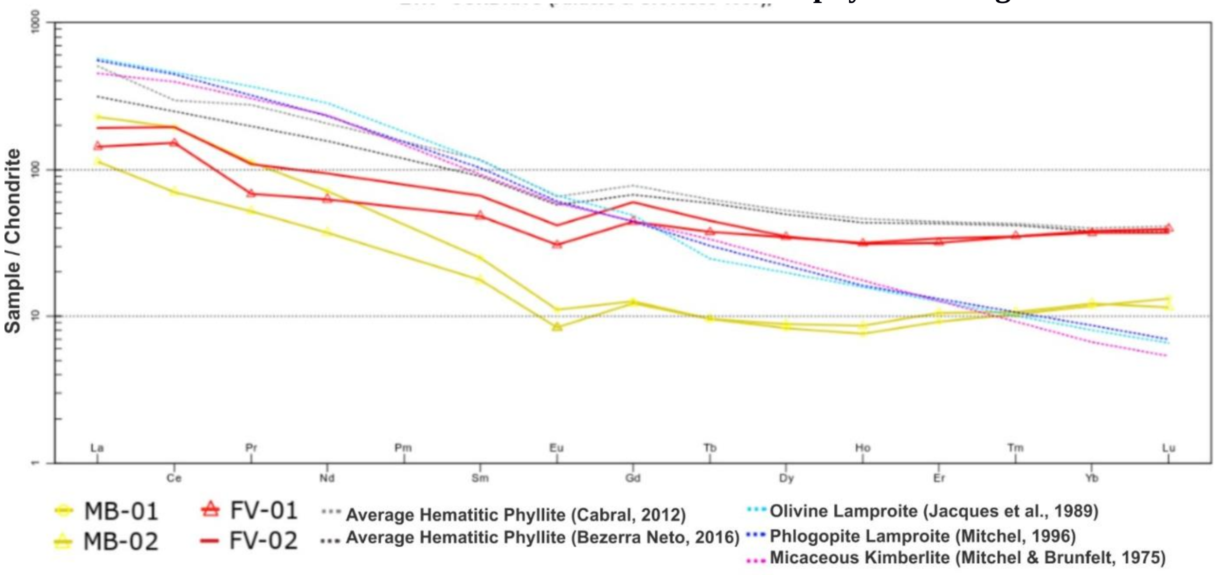

The REE patterns obtained for quartzite breccias and reddish phyllites were compared with the average patterns of hematitic phyllites (Bezerra Neto, 2016; Cabral *et al.*, 2012), olivine lamproites, phlogopite lamproites (Mitchell and Bergman, 1991) and micaceous kimberlites (Mitchell and Brunfelt, 1975) (Figure 10). The breccias present a negative gap in relation to the HREE when compared to hematitic phyllites and reddish phyllites, presenting a LREE fractionation similar to hematitic phyllites. The correlation index of the breccias with the

https://doi.org/10.5281/zenodo.17553543

hematitic phyllites is 0.95, demonstrating a strong correlation despite the mentioned negative gap.

7. Discussions

7.1 What is the origin of diamond-bearing quartzite breccias?

The quartzite breccias of the SBf were discovered as diamond-bearing rocks in the Barro mine in 1840, and their igneous origin has been advocated since Thompson (1928). The controversial origin of these breccias, i.e., their geological environment, arises from the characteristics of the place where they occur, the geometry of the bodies and, above all, in view of their petrography, mineralogy and lithogeochemistry and diamond mineralization itself. Petrographically, they are defined as quartzite breccias containing quartzite/metarenite clasts of varying dimensions (submillimetric to over 50 cm), predominantly red to pink in color, and very angular, therefore a clear indication of a proximal source. The homogeneity in the distribution of the red or pink color of the clasts, i.e., without concentric variations or intensity from the edges to the center, indicates that the event responsible for the oxidation occurred before the removal of the clasts from the original layers. Phyllitic matrix predominates, occasionally with the terms arenopelitic or sandy. The rock itself, and especially the matrix, is highly weathered and therefore the phyllitic material is transformed into clay minerals, especially kaolinite. Diamonds appear as xenocrysts and vary in size from submillimetric to a few centimeters. At least eight diamonds weighing 30 ct or more have been recovered (not counting gems extracted from drainages that arise over mines containing breccias) in the Pagão, Campo Sampaio Novo, João Boa and MCN mines (Renger *et al.*, 2025). The shape and thickness of the bodies vary from a few meters to several tens of meters, forming irregular bodies, sometimes in the shape of a “champagne glass” (Miranda *et al*. 2019). Breccia bodies of submetric dimensions, intrusive, subvertical, embedded in the metarenites and phyllites of the sedimentary succession were identified in the Caldeirões mine (Almeida-Abreu and Renger, 2001) and in the MCN (Miranda *et al*. 2019).

As previously mentioned, the chemistry of the breccia matrix does not reveal a composition compatible with rocks of an igneous nature, except for the rare earth elements that fall in the field of rocks of a kimberlite nature. The quartzite breccia bodies (always diamondiferous) occur in the mines of João Boa, Córrego Novo, Campo Sampaio, Água Fria, Pagão, Pagãozinho and Barro (District of São João da Chapada-Campo Sampaio), also showing bodies to the south, that is, the mines that, aligned in the N-S direction, continue to the District of Sopa-Guinda

https://doi.org/10.5281/zenodo.17553543

(mines of João Dari and Morrinhos), and, in this last district, they appear as robust bodies in the mines of Caldeirões, Chalé, Sopa, Barro Branco and Brumadinho. To the south of the district of Sopa-Guinda they also appear as smaller occurrences at the foot of the Serra do Pasmar, to the south of Barão do Guaicuí and in the locality of Chapadinha (Gouveia). They are therefore distributed over a north-south extension of approximately 50 km (Figure 1). In the mines of the Sopa-Guinda district, the breccias are located near the top of the unit, but the same formation presents, in its lower part, many bodies of diamondiferous orthoconglomerates.

At the Barro Mine (São João da Chapada), drilling cores recovered samples of breccia bodies at depths of up to 60 meters without reaching the bedrock (Thompson, 1928). The breccias and associated phyllites are circumscribed by quartzite rocks in well-defined contacts and with steep dips, suggesting that the breccias are contained in narrow depressions in a N-S direction, modeled in the quartzites, thus configuring themselves as craters.

Thompson (1928) is emphatic in stating that the "breccias are evidently of igneous origin, as shown by (a) the mode of occurrence; (b) the character and distribution of the included fragments; (c) the occurrence in the matrix of minerals in a fresh state, undoubtedly of primary origin; (d) the proven identity of the matrix material with that of the associated dikes, which are certainly igneous". Furthermore, it highlights that neither the diamonds nor the associated minerals recovered from the breccia matrix present the usual signs of wear in alluvial deposits and that the diamonds are found only in the breccia matrix and, further, that the breccia diamonds present peculiar and consistent characteristics for each deposit, in contrast to the mixed characteristics presented by those of alluvial deposits. In an outcropping dike at the Barro Mine, Thompson (1928) indicated, through qualitative tests, the high percentage of magnesium and the great abundance of iron and titanium minerals, which would indicate a rock of a basic and non-acidic nature and suggests, finally, that the breccias of the Diamantina district are sources of diamonds analogous to those of the pipes of South Africa.

Mineral inclusions in MCN diamonds indicate that these diamonds originated in the peridotite lithospheric mantle, while their perfectly preserved physical features, unlike diamonds extracted from the Jequitinhonha River - which show conspicuous signs of abrasion due to river transport - reveal that the breccia gems did not undergo any sedimentary reworking (Müller, 2021). The mineral inclusions recognized in these diamonds, as well as in diamonds studied by other authors (see references in Muller, 2021) indicate their mantle affinity and that they were carried to the surface by rocks of a kimberlitic nature.

From the above, there seems to be no doubt that the breccias are of igneous origin, generated in situ by explosive kimberlite volcanism (phreatomagmatic – favored by water saturation in

ISSN 2317-0611

sedimentary successions, according to the humid climate). The disturbances inherent to phreatomagmatic processes promoted the erosion of the host rocks and the generation of maar craters on the alluvial plain, eventually forming shallow and not very extensive lakes.

So why, then, do these breccias not have clasts of kimberlites, classic satellite minerals of diamonds and even clasts of basement rocks as in breccias of a similar nature in kimberlites from different places?

7.2. *The Paleo-Mesoproterozoico climate regime*

Discussions about the climatic conditions at the end of the Paleoproterozoic and in the Mesoproterozoic were summarized by Almeida Abreu (1993), according to the high atmospheric CO_2 rates of the Precambrian to explain the warmed earth in the spectrum of the faint sun paradox, when he admitted that the successions of the Espinhaço Supergroup were deposited under permanent conditions of a hot and humid climate. He then referred to the compositional maturity of the sediments of the Guinda Group recorded throughout the SER (Almeida Abreu, 1993; Almeida Abreu and Renger, 2001, 2007) as indicative of these hot and humid climate conditions and of expressive weathering efficiency. The recognition of hematitic phyllites that are exposed in different areas of the SER as paleo-laterites/-bauxites from the alteration of synsedimentary basic volcanic rocks, metamorphosed during the Espinhaço orogeny (Knauer and Schrank, 1993), also testifies to these "tropical climate" conditions.

More recent studies have confirmed that Precambrian climatic conditions presented suis generis characteristics when compared to Phanerozoic conditions. Medaris Jr *et al*. (2021), for example, admitted that Mesoproterozoic sedimentary rocks from the southern Lake Superior region (≤1.63 Ga) are "among the most mature in the geological record", as per the occurrence of conglomerate with quartz and ferricrete or jasper pebbles without containing clasts of underlying lithologies or detrital feldspars, as well as the presence of metamorphosed kaolinite and, furthermore, the identity of the chemical maturity revealed by the Chemical Alteration Index (CIA) of associated pelitic layers, which would have been generated under warm and humid climatic conditions.

Retallack and Schmitz (2023), in turn, suggested the occurrence of acid rain (pH 4.0–4.5) due to the high atmospheric CO_2 content in the Archean, also indicating that weathering could have been enhanced by biogenic sulfuric acid present in soil water, reducing the pH to values of 2–3, which would then promote the generation of more soils. Although they considered maximum atmospheric CO_2 levels of only 11.3 ± 1.6 to 8.8 ± 0.5 times compared to pre-industrial atmospheric levels (PAL), they emphasized the imperative need for other gases

https://doi.org/10.5281/zenodo.17553543

ISSN 2317-0611

(water vapor, CH_4, C_2H_6, SO_2 and OCS) to be present in the atmosphere to maintain a greenhouse effect adequate to sustain a warm climate under conditions of the Archean solar energy rate.

Kah and Riding (2007) concluded, from the study of cyanobacteria, that atmospheric pCO_2 at the end of the Mesoproterozoic would have levels ≤10 PAL (estimating values of 7-10 PAL), which would require the presence of other greenhouse gases to raise the temperature under lower solar luminosity and, therefore, indicate the presence of 100–200 ppm of methane in the Mesoproterozoic atmosphere. A similar indication of lower atmospheric CO_2 rates in Precambrian relative to the initial models to overcome the faint sun paradox was proposed based on studies of Archean and Mesoproterozoic paleosol proxies by Sheldon *et al*. (2021), but they emphasized the indispensable presence of other greenhouse gases in the Precambrian atmosphere, probably CH_4 or N_2O.

From another perspective, Bayon *et al*. (2022) proposed that the long-term increase in terrestrial chemical weathering was associated with atmospheric O_2 levels throughout Earth's history, as per direct evidence of the onset of terrestrial weathering during the late Archean to early Paleoproterozoic, after the emergence of large continental masses, further highlighting that terrestrial chemical weathering may have been fundamental in driving the long-term evolution of the Earth's biosphere.

Recent studies therefore reiterate Precambrian climate regimes with significant differences from Phanerozoic climate regimes and highlighted, even more, by the (in)existence of components that substantially influence the climate, that is, the absence of vegetation cover on the continents, the size and distribution of continental areas, hypsography and thermodynamic relations of the crust-mantle system that directly influence the continental freeboard and this plays a relevant role in the intensity of leaching processes, given that the relief and the time of exposure of the rocks are components that influence the dissolution rates of the minerals.

How efficient or deleterious would meteoric waters and other sources of the hydrosphere be in the processes of transformation and dissolution of rocks, i.e., weathering, under the climatic conditions of the Proterozoic? Not only the very humid climate conditions themselves, and the pCO_2 of the order of 10 times the PAL, but also the meteoric solutions after the dissolution of gaseous components of the atmosphere such as CH_4, C_2H_6, SO_2, N_2O and OCS?

As summarized above, humid climatic conditions in different geological provinces of the Precambrian are well recorded, and the very humid climatic conditions during the deposition of the Espinhaço Supergroup units also have robust records (Almeida Abreu 1993), such as the concentration or deposits of kaolinite in successions of the São João da Chapada and Sopa

https://doi.org/10.5281/zenodo.17553543

Brumadinho formations, the extensive presence of laterization products (i.e., hematitic phyllites), the general absence of rocks rich in labile minerals, the compositional maturity of rudite clasts, and, of course, the Chemical Alteration Index (CIA). Certainly, the composition (acidity) of meteoric waters played a greater role in the weathering processes and, considering the high levels of atmospheric CO_2 and other gases that contributed to the acidity of meteoric waters, the efficiency over time and in the profile of rock/soil weathering would have been maximized in Precambrian times.

Diamond processing operations from breccias in the region's mines invariably show very small quantities of heavy residual minerals when compared with the residual concentrates of conglomerates that occur in the lower strata of the same formation. Iron oxides and hydroxides (hematite, magnetite, goethite, martite) predominate, and rutile prisms are also present, i.e., no minerals characteristic of primary diamond rocks appear. However, the abundant minerals in the residues of the concentrates of both conglomerates and breccias are not labile minerals. On the contrary, they are stable minerals related to weathering in the Goldich series, and even the preserved translucent minerals are generally tourmaline, zircon and rutile, which make up the top of the mineralogical maturity index (ZTR). Even in the Extraction District conglomerates, where proximal source areas are indicated by angular clasts and abundant grains of plagioclase and potassium feldspar, granitoid clasts are virtually absent, as are the metamorphic rocks that contained the milky quartz vein clasts. Decimetric (subangular) quartzite clasts with primary (pre-depositional) ferruginous concretions were also identified in the Extraction District conglomerates, strongly demonstrating humid climatic conditions.

Based on the above, the absence of clasts and minerals typical of the primary diamond rocks that mineralized the breccias cannot be considered a paradox, although there is still (or persists) some mystery regarding the geological evolution of the SBf diamond breccias.

7.3. *Breccias and their origin from phreatomagmatic volcanism*

There seems to be a consensus regarding the recognition of significant variations in volcanic processes related to kimberlitic magmatism, which presents specificities such as magma volumes per event and the different natures of the host rocks and, in addition, the occasional (and relevant) influence of groundwater and other underground sources on phreatomagmatic processes. Furthermore, would kimberlite magmas have maintained the same nature since the Precambrian, considering the secular changes in mantle temperature and the pervasive (and increasing – since the Archean) influence of the recycling of lithospheric plates after subduction (Lai *et al*., 2023, Regier *et al*., 2023)? The existence of different volcanic facies between the

ISSN 2317-0611

Ekati (Canada) and southern African pipes, supposedly due to specific eruptive episodes, is reported by Porrit *et al*. (2008). These authors also argue that most of the breccias within the kimberlite pipe originate from the collapse of the pipe wall and that during an explosive eruption, the magma is fragmented due to the expansion and coalescence of the gas with increased shear stress and deformation rate created in the conduit during rapid upward acceleration. In turn, the explosive emplacement of kimberlites from the Diavik mine (Northwest Territories, Canada) was triggered by increased groundwater availability, changes in the local stress field and/or variables in the magma supply rate, without any control of the magma composition (Tovey *et al*., 2020).

The studies and analyses of the MCN breccias, as explained above, demonstrate a magmatic origin under phreatomagmatic volcanism, which brings with it another question: where are the ducts that carried the magmatic solutions to the surface? Yes, several (many dozens) of narrow dikes (millimetric to decimetric thick) of more or less kaolinized “phyllites” appear embedded in the quartzites of the bedrock (Figure 5), including a swarm of anastomosing dikes indicating the embryonic process of fragmentation of the quartzites' substrate for the formation of breccias (Figure 5c). These dikes were subjected to the compressive deformation of the Espinhaço Orogeny and, consequently, severely thinned and even strangled, that is, they could originally have had submetric or even metric thicknesses.

Note that in the Fort à la Corne kimberlite volcanic complex (Saskatchewan, Canada), even though these rocks are of Upper Cretaceous age, the location and configuration of the volcanic conduits of its kimberlite packages emplaced in a continental and marginal marine basin are not known (Pittari *et al*., 2008). This kimberlite volcanic complex of Central Orion shows other similarities with the MCN breccia complex: (1) crater excavation processes comparable to those of phreatomagmatic maars that emerged from paleoaquifers; (2) craters filled with volcaniclastic deposits soon after their formation, during the same eruptive event; (3) unidentified volcaniclastic input (pyroclastic deposition, reworked epiclastics) within the stratified rock facies association, perhaps because they were extensively altered; (4) extensive alteration of stratified packages, preserving few textural details to identify volcanic facies characteristics.

In the model of the evolution of phreatomagmatic magmatism by Kurszlaukis and Lorenz (2008) magma ascends to a first explosion near the surface and may create a relatively wide and shallow maar crater. The energy for the pipe excavation process must originate from magma ascending from the very thin (<1 m) feeder dike to the basal part of the root zone, which is the deepest point of explosive activity in a pipe. In smaller pipes, as a consequence of strong

https://doi.org/10.5281/zenodo.17553543

explosions, the entire tephra column at the diatreme may be affected and partially or completely fluidized at temperatures between 200 and 450 °C, and the heated groundwater will alter the existing minerals (e.g. olivine to serpentine) and may also dissolve certain minerals (e.g. carbonate) and fayalite is altered to magnetite and dissolved H_2 and SiO_2.

The breccias of the São João da Chapada – Campo Sampaio Diamond District are located on a plateau at approximately 1,400 meters asl, and are located, along with the other lithologies that accompany them, in relatively shallow depressions with a N-S to NNW-SSE orientation, ranging in length from 350 to 1,300 meters and widths between 200 and 600 meters (these crater-depressions are certainly flattened by compressional tectonics, with narrowing of their E-W sections). The succession of sandstones of the São João da Chapada Formation that surrounds the breccias and associated lithologies, according to the escarpments that surround the plateau, has an outcrop thickness of around 250 meters. Therefore, this is the minimum thickness of sedimentary rocks that were traversed by the conduits of phreatomagmatic volcanism for the formation of the craters and subsequent "deposition" of the diamond-bearing breccias in these troughs. The total thickness of the sedimentary succession beneath the craters may be greater than 250 meters, since a thick sill of basic rocks of the Pedro Lessa Suite (post-tectonic related to the SER orogenesis) is located beneath the outcropping succession of the São João da Chapada Formation around the plateau. However, it is likely that this sill is located at the interface of the sedimentary cover with the crystalline substrate, i.e., the pre-Espinhaço basement.

As mentioned, Kurszlaukis and Lorenz (2008) propose that magma rises through rocks to shallow levels and in a first explosion close to the surface it can create a relatively wide and shallow crater and only through successive explosions does a diatreme develop which, in a continuous process, deepens and widens the crater with the formation of classic carrot-shaped diatremes. As magma rises to shallow levels, the level of neutral buoyancy can be reached due to the loss of volatile when the ascent speed decreases and sills can form and, in this case, with the cooling of the pressurization, the processes typical of phreatomagmatic volcanism cease.

Apparently, in the mines of the Diamond District of São João da Chapada – Campo Sampaio, only the first explosion occurred in the context of the phreatomagmatic volcanic evolution that would lead to the development of classic diatremes. Why? Could these magmas be somewhat deficient in volatiles?

From this perspective, according to the presence of flat-bottomed trigons in the diamonds of the district, there would have been interactions with magmas rich in H_2O during the final stages of the ascent (Müller, 2021), which may have led to the loss of volatiles through chemical

https://doi.org/10.5281/zenodo.17553543

ISSN 2317-0611

reactions. A low water table saturation of the sedimentary succession seems unlikely according to the indications of a humid climate, but in the case of sandy sedimentary rocks, therefore very porous (especially when poorly consolidated), it could lose significant volumes of water vapor due to the heating effect of the kimberlitic fluids (temperatures of up to 450°C inside the diatreme are reported by Kurszlaukis and Lorenz, 2008). It can also be assumed that the high porosity of the host sedimentary succession could dissipate a significant part of the volatiles during the ascent of the magma, as the pores are emptied by the loss of water vapor.

8. When, Where and Why Diamonds Were Formed

The transition from the Archean to the Proterozoic at ~2.5 Ga has been considered as the apogee of the formation of cratonic cores, which represent most of the surface of the present-day Earth's crust. However, Mazumder *et al*. (2019, 2022) report two major changes in the Neoarchean: the cooling of the mantle and the stabilization of major cratons at 2.7 to 2.5 Ga, highlighting even, based on the occurrence of a 3.2 Ga paleosol and alluvial deposits on the Singhbhum craton (India), higher continental freeboard already prevailed during the Neoarchean. Retallack *et al*. (2023) also reported the presence of paleosols on an Archean craton (3.3 Ga) in western Australia.

On the other hand, Hawkesworth *et al*. (2020, and references therein) proposed a reduction in crustal growth rate at ~3 Ga, suggesting a change in the processes of generation and/or preservation of the crust due to the advent of plate tectonics as the dominant process of crust generation. They also referred to the compilation of isotopic and bulk chemical data of silicate and sulfide inclusions in diamond with peridotitic composition before 3.2 Ga, whereas after 3.0 Ga eclogitic inclusions became prevalent. The eclogitic inclusions are considered to arise from the subduction of mafic material, and hence to the onset of plate tectonics, further suggesting that by 3 Ga the volume of continental crust was between 65% and 70% of its present-day volume.

Smit *et al*. (2022, and references therein) referred as an updated definition of a craton, “regions of the Earth's continental crust that are underlain by 150–200 km thick continental lithospheric mantle providing long-term stability since at least 1 Ga, therefore, around 63% of exposed continental crust and 18% of Earth's surface can be considered as cratonic”.

Pintér *et al*. (2022) pointed out that the thick mantle lithosphere beneath the cratons — the ancient cores of the continents — has cold, stable roots reaching ~250 km depth, which consists of strongly reduced rocks that have reacted with oxidized incipient melts with low-silica, and

https://doi.org/10.5281/zenodo.17553543

ISSN 2317-0611

rich in CO_2 and H_2O. The reaction of the melts with the surrounding rocks forms an enriched zone at the base of the lithosphere, which is the source region for many diamonds.

Diamonds reside in the lithospheric mantle beneath cratons, and the intersection of peridotite derived conductive geotherms with the diamond stability field, led to the suggestion that diamonds have formed through nearly all of Earth's history in distinct episodes that can often be linked to larger-scale tectonic processes (Smit *et al*. 2022).

Most diamond inclusion minerals originate in the sub-continental cratonic mantle lithosphere and only a small percentage of mineral inclusions originate beneath the lithosphere (~1%, Stachel and Harris 2008). Inclusions in diamonds are classified as protogenetic (preceding diamond formation), syngenetic (cocrystallizing with diamond) or epigenetic (crystallizing after diamond formation). Typically, a syngenetic origin for inclusions has been inferred if, regardless of their crystal system, the inclusions show a cuboidal-octahedral morphology that is imposed by their diamond hosts, which is most commonly the case (Walter *et al*. 2022). The fluid inclusions trapped in fibrous diamonds from the lithosphere report that the parental fluids exhibit a range in composition, including high- and low-Mg carbonatitic, chlorine-rich and silica-rich aqueous fluids (Walter *et al*. 2022).

Repeated episodes of crystallization and/or additional diamond growth have occurred in mantle domains of diamond stability throughout much of Earth's history, primarily in the lithospheric upper mantle beneath primitive continental cores, but also in the asthenosphere and in tectonically activated crustal rocks, phenomena associated with subduction-related melt generation, migration of metasomatic fluids, and reaction with preexisting peridotite, eclogite, and websterite in the mantle (Gurney *et al*., 2010). The major Archean crystallization of smooth crystalline diamonds in the Kaapvaal, Slave and Siberian cratons in metasomatized harzburgite provides evidence that by 3 Ga stable, buoyant, chemically depleted and reduced continental craton cores extended to depths at temperatures at which diamonds can be stable and stored for long periods of geological time. The subsequent formation of smooth crystalline diamonds in the subcontinental lithospheric mantle is closely associated with the establishment of these early craton cores. Fibrous cuboidal diamonds and fibrous layers in smooth crystalline diamonds are also of metasomatic origin, growing as xenocrysts in the same lithospheric mantle, but with much shorter mantle residence times, typically <5 million years. Their formation, shortly before sampling and magmatic transport to the crust, suggests that they represent a final burst of diamond formation as metasomatic influx of volatile components increased in the lithosphere prior to the kimberlite eruption (Gurney *et al*., 2010).

https://doi.org/10.5281/zenodo.17553543

ISSN 2317-0611

Despite the occurrence (sometimes abundant) of microdiamonds and macrodiamonds (the latter occurring locally and always smaller than 3 ct) in rocks from the Archean and Lower to Middle Paleoproterozoic (Gurney *et al*., 2010), diamonds larger than 5 ct appear only in the late Paleoproterozoic (Statherian Period), precisely in cratonic areas of Brazil (Roraima and Espinhaço Range), which, therefore, reports the Diamond Province of the SER as the oldest in the history of the Earth. On the other hand, diamonds larger than 150 ct have their advent with the emergence of "CLIPPIR" (Cullinan-like, Large, Inclusion-Poor, Pure, Irregular, and Resorbed) around 1200 Ma (Stenian Period of the Mesoproterozoic), specifically in the Premier Kimberlite of South Africa (Gurney *et al*., 2010). Diamonds of 400 ct and larger have been found in diamond provinces of the Paleozoic (Siberia), Mesozoic (in different countries of Africa and in western Minas Gerais) and Cenozoic (Canada) (Kjarsgaard *et al*., 2022).

Diamonds in detrital rocks aged between 3.3 and 3.5 Ga found in the Slave craton (Canada) show a combination of high $\delta^{13}C$ and $\delta^{15}N$ values, demonstrating that marine crustal carbonate was present in the source, brought to depths >170 km, possibly through subduction processes (Timmerman *et al*., 2022). This leads to the assumption that diamonds are formed primarily by the supply of organic carbon from the crust through recurrent subduction processes, thus allowing us to conjecture that the increase in the quantity and size of diamonds throughout Earth's history was due to the increasing incorporation of segments of oceanic crust into the mantle environment. In this case, the advent of robust diamond deposits with crystals measuring centimeters to decimeters from the end of the Paleoproterozoic (Zhang *et al*., 2024), which then includes the Diamond Province of the SER, and especially of the Mesoproterozoic era (Premier kimberlite and Argyle lamproite) and the subsequent growth in the quantity and volume of diamond deposits during the Phanerozoic, would not have been fortuitous.

In a tight synthesis, it can be concluded that diamonds from the subcontinental lithosphere are formed under the metasomatism of carbonatitic or carbonated silicate melt (Babu *et al*. 2023). A somewhat similar conclusion was reached by Pintér *et al*. (2022) through experimental work, when they observed that the thick mantle lithosphere beneath cratons consists of strongly reduced rocks that have reacted with oxidized melts. The low-silica incipient melts are rich in CO_2 and H_2O and react with surrounding rocks forming an enriched zone at the base of the lithosphere, which is the source region for many diamonds. Also referred to as an alternative mechanism to subducted or delaminated crust, or underplating by voluminous silicate magmas for the formation of pyroxenitic garnet and clinopyroxene inclusions in some lithospheric diamonds.

https://doi.org/10.5281/zenodo.17553543

ISSN 2317-0611

9. Conclusions

In the SER and adjacent domains, diamonds are not known in Precambrian rocks or successions prior to (or subsequent to), the deposition of the SBf, a fact that allows us to conclude: (1) kimberlitic volcanism occurred at approximately 1.7 Ga, considering the ages obtained in synsedimentary volcanic rocks intercalated in the SBf (Dossin *et al*., 1993; Hagedorn, 2004; Bezerra-Neto, 2016); (2) this age therefore reveals that the diamond province of the SER is the oldest in Earth's history, since those of Argyle and Premier are from the Mesoproterozoic (Smit *et al*., 2022); (3) the intrinsic crustal instabilities of the SBf, according to its rudite deposits related to tectonic movements throughout the edge of the sedimentary basin, establish a cause and effect relationship with kimberlitic magmatism.

The SBf breccias are located in successions at the top of the unit and show notable characteristics of in situ formation or very proximal sources, while the conglomerates that make up the lower successions of the unit have, in most of their clasts, characteristics of somewhat distant provenance, that is, tens of kilometers to the W (Renger *et al*., 2025), therefore, at least two generations of kimberlitic magmatism occurred in the SER.

The intersection of structural lineaments of significant regional extent, i.e., those with a NNW-SSE orientation with the lineament bundles with a NE-SE and WNW-ESE orientation (Figure 8) within the São João da Chapada – Campo Sampaio Diamond District, as well as in the Diamond Extraction District, stand out as the crustal-lithospheric structures that provided the kimberlite magmatism of the diamond province of the SER.

Despite composing deposits of a suis generis character when compared to the occurrences of breccias and associated rocks of kimberlite extrusions in other regions of the planet, the diamond-bearing breccias of the SER, especially those of the MCN, evoke the geological environment of maar craters typical of kimberlite volcanism, because: (1) all their occurrences within the SER are diamond-bearing (including gems of up to 38 ct) and mineral inclusions of their diamonds show affinity with peridotite rocks; (2) the breccias and associated deposits are housed in depressions shaped in quartzite rocks that surround them, configuring narrow and elongated troughs (craters); (3) the rocks that generated the clasts, i.e., quartzites (often reddish), compose the substrate of the breccia mines; (4) the pelitic and areno-pelitic successions that cover the breccias show sedimentary arrangements and structures characteristic of aggradational deposition in a lacustrine environment; (5) hundreds of narrow "phyllite" dikes permeate the quartzites of the substrate that support the breccias, and must represent alteration products (hydrothermal and weathering) of fluids ejected by

https://doi.org/10.5281/zenodo.17553543

phreatomagmatic volcanic processes; (6) although rare, breccia dikes embedded in arenites/pelites exposed in the Caldeirões and Córrego Novo mines have been recognized.

Another suis generis characteristic of the geology of SBf breccias is their ubiquity in economic diamond mineralization, which gives the respective source rocks (kimberlites) good prospects for economic grades.

References

Alkmim, F. F.; Martins-Neto, M. A. (2012). Proterozoic first-order sedimentary sequences of the São Francisco craton, eastern Brazil. **Marine and Petroleum Geology**, 33(1), p. 127–139.

Almeida, F. F. M. (1977). O Cráton do São Francisco. **Revista Brasileira de Geociências**, 7(4), p. 349–364.

Almeida-Abreu, P. A. (1993). A Evolução Geodinâmica da Serra do Espinhaço Meridional, Minas Gerais, Brasil. Tese de Doutoramento, University Freiburg (Alemanha).

Almeida-Abreu, P. A. (1995). O Supergrupo Espinhaço da Serra do Espinhaço Meridional (Minas Gerais): o Rifte, a Bacia e o Orógeno. **Geonomos**, 3(1), p. 1–18.

Almeida- Abreu P. A. (1996). O caminho das pedras. **Geonomos**, 4(1), 77-93.

Almeida-Abreu, P. A.; Renger, F. E. (1999). Discussão: "Sobre a polêmica da origem do diamante na Serra do Espinhaço (Minas Gerais): um enfoque mineralógico", de M. L. de S. C. Chaves, J. Karfunkel e D. P. Svisero. **Revista Brasileira de Geociências**, 29, p. 669–672.

Almeida-Abreu, P. A., Renger, F. E. (2001). A origem dos diamantes da Serra do Espinhaço Meridional: o exemplo do distrito diamantífero de Sopa-Guinda (Diamantina, MG). **Revista Brasileira de Geociências**, 31 (4), p. 511–520.

Almeida-Abreu, P. A.; Renger, F. (2002). Serra do Espinhaço Meridional: um orógeno de colisão do mesoproterozóico. **Revista Brasileira de Geociências**, 32 (1), p. 1–14.

Almeida-Abreu, P. A., Renger, F. E. (2007). Stratigraphy and facies of the southern Serra do Espinhaço, Minas Gerais, Brazil. **Zeitschrift der deutschen Gesellschaft für Geowissenschaften**, 158 (1), p. 9-29.

Amaral-Santos, E.; Jelinek, A. R.; Almeida-Abreu, P. A.; Genezine, G. A. (2019). Phanerozoic cooling history of Archean/Paleoproterozoic basement in the southern Espinhaço Range, southeastern Brazil, through apatite fission-track analysis. J. S. Amer. **Earth Sciences**, 96(102352). https://doi.org/10.1016/j.jsames.2019.102352.

Anders, E.; Grevesse, N. (1989). Abundances of the elements: meteoric and solar. **Geochimica et Cosmochimica Acta**, 53, p. 197-214. https://doi.org/10.1016/0016-7037(89)90286-X.

Babu, E. V. S. S. K.; Dash, S.; Santhosh, G. H. N. V.; Mukherjee, A. (2023) Origin of clinopyroxene megacrysts from the 1.1 Ga Chigicherla-4 kimberlite (CC4), Dharwar craton, southern India: Implications for multi-stage metasomatism of the sub-continental lithospheric

ISSN 2317-0611

mantle. **Journal Asian Earth Science**, 244(105534). https://doi.org/10.1016/j.jseaes.2022.105534.

Bayon, G.; Bindeman, I. N.; Trinquier, A.; Retallack, G. J.; Bekker, A. (2022). Long-term evolution of terrestrial weathering and its link to Earth's oxygenation. **Earth and Planetary Science Letters**, 584(117490).

Bezerra Neto, F. E. (2016). Estudo de rochas exóticas da Formação Sopa-Brumadinho e possíveis implicações para a fonte dos diamantes do Espinhaço Meridional. Dissertação de Mestrado. IGeo - Universidade de Brasília.

Cabral, A. R.; Wiedenbeck, M.; Koglin, N.; Lehmann, B.; Abreu, F. R. (2012). Boron-isotopic constraints on the petrogenesis of hematitic phyllite in the southern Serra do Espinhaço, Minas Gerais, Brazil. **Lithos**, 140(141), p. 224-233.

Caldas, J. P. P.; Chaves, M. L. S. C.; Barbosa, M. S. C. (2019). Anomalias magnetométricas da região de Diamantina (Serra do Espinhaço, Minas Gerais) e seus significados geológicos, estruturais e tectônicos. **Geociências (UNESP)**, 38(4), p. 871 – 885.

Chaves, A. O. (2013). Enxames de diques máficos de Minas Gerais – O estado da arte**.** **Geonomos**, 21(1), p. 29-33.

Chaves, A. O.; Neves, J. M. C. (2005). Radiometric ages, aeromagnetic expression, and general geology of mafic dykes from southeastern Brazil and implications for African-South American correlations. **Journal of South American Earth Science**, 19, p. 387-397.

Chaves, A. O.; Ernst, R. E.; Söderlund, U.; Wang, X.; Naeraa, T. (2019). The 920 900 Ma Bahia-Gangila LIP of the São Francisco and Congo cratons and link with Dashigou-Chulan LIP of North China craton: new insights from U-Pb geochronology and geochemistry. **Precambrian Research**, 329, p. 124–137.

Chaves, M. L. S. C. (1997). Geologia e mineralogia do diamante da Serra do Espinhaço em Minas Gerais. Tese de Doutorado, São Paulo, IG-USP, 289 p.

Chaves, M. L. S. C.; Karfunkel, J.; Svisero, D. P. (1998). Sobre a polêmica da origem do diamante na Serra do Espinhaço (Minas Gerais): um enfoque mineralógico. **Revista Brasileira de Geociências**, 28, p. 295-294.

Chaves, M. L. S. C.; Karfunkel, J.; Svisero, D. P. (1999). Réplica da discussão de P. Almeida-Abreu and F. Renger – Sobre a polêmica da origem do diamante na Serra do Espinhaço (Minas Gerais): um enfoque minerológico. **Revista Brasileira de Geociências**, 29, p. 673-674.

Chemale Jr., F.; Dussin I. A.; Alkmim, F. F.; Martins, M. S.; Queiroga, G.; Santos M. N. (2012). Unravelling a Proterozoic basin history through detrital zircon geochronology: The case of the Espinhaço Supergroup, Minas Gerais, Brazil. **Gondwana Research**, 22(1), p. 200–206.

CODEMIG - Companhia de Desenvolvimento Econômico de Minas Gerais (2012). Mapa Geológico 1:100.000 (Fls. Conceição do Mato Dentro, Curimataí, Diamantina, Presidente Kubitschek, Serro, Rio Vermelho). Projeto Criação de Banco de Dados Geográfico para os

Mapas Geológicos do Projeto Espinhaço, Minas Gerais, Versão SIG, Laboratório de Mapeamento Geológico Digital–MGD. http://www.portalgeologia.com.br/index.php/ mapa/.

Correns, C. W. (1932). Die Diamanten des Hochlandes von Minas Geraes, Brasilien**. Zeitschrift für praktische Geologie**, 40(11), p. 161-176.

CPRM-CODEMIG (2014). Mapa Geológico do Estado de Minas Gerais, Escala 1:1.000.000. Ministério das Minas e Energia, Secretaria de Geologia, Mineração e Transformação Mineral. Edição atualizada, dezembro/2014.

D'Agrella-Filho, M. S.; Pacca, I. G.; Teixeira, W.; Onstott, T. C.; Renne, P. R. (1990). Paleomagnetic evidence for the evolution of Meso- to Neoproterozoic rocks in central-eastern Brazil. **Palaeography, Palaeoclimatology, Palaeoecology**, 80, p. 255–265.

Dossin, I. A.; Dossin, T. M.; Chaves, M. L. S. C. (1990). Compartimentação estratigráfica do supergrupo Espinhaço em Minas Gerais - os grupos Diamantina e Conselheiro Mata. **Revista Brasileira de Geociências**, 20(1-4), p. 178–186.

Dossin, I. A.; Dossin, T. M.; Charvet, J.; Cocherie, A.; Rossi, P. (1993). Single-Zircon dating by step wise Pb-evaporation of Middle Proterozoic magmatism in the Espinhaço Range, southeastern São Francisco Craton (Minas Gerais, Brazil). 2° Simpósio do Cráton São Francisco, Salvador, **Anais**, SBG, p. 39-42.

Dossin, I. A.; Uhlein, A.; Dossin, T. M. (1984). Geologia da Faixa Móvel Espinhaço em sua porção meridional, MG. 33º Congresso Brasileiro de Geologia, 2, Sociedade Brasileira de Geologia 2, p. 3118–3132.

Guadagnin, F.; Chemale Jr. F. (2015). Detrital zircon record of the Paleoproterozoic to Mesoproterozoic cratonic basins in the São Francisco Craton. **Journal of South American Earth Sciences**, 60, p. 104–116.

Garcia, A. J. V.; Uhlein, A. (1987). Sistemas deposicionais do Supergrupo Espinhaço na região de Diamantina (MG). Simpósio sobre Sistemas Deposicionais no Pré- Cambriano, Ouro Preto, SBG, p. 113-135.

Gurney, J. J.; Helmstaedt, H. H.; Richardson, S. H.; Shirey, S. B. (2010). Diamonds through Time. **Economic Geology**, 105, p. 689–712.

Hagedorn, M. G. (2004). Contexto Geotectônico da Serra do Espinhaço e domínios adjacentes a leste (Minas Gerais) com ênfase em aspectos geoquímicos e geocronológicos. Tese de doutorado, Instituto de Geociências e Ciências Exatas, Universidade Estadual Paulista, Rio Claro-SP.

Hawkesworth, C. J.; Cawood, P. A.; Dhuime, B. (2020). The evolution of the continental crust and the onset of plate tectonics. **Frontiers in Earth Science**, 8. https://doi.org/10.3389/ feart.2020.00326.

Hoppe, A. (1986). Geodynamic evolution of an Early to Mid-Proterozoic mountain range: The Serra do Espinhaço, central-eastern Brazil. Geocongress '86-21, Johannesburg, Biannual Congress Geology of South Africa, Extended Abstracts, p. 307- 309.

Jaques, A. L.; Haggerty, S. E.; Lucas, H.; Boxer, G. L. (1986). Mineralogy and petrology of the Argyle (AKI) lamproite pipe, Western Australia. **International Kimberlite Conference, Perth, Extended Abstracts**, 4(1), p. 48–50. https://doi.org/10.29173/ikc1069.

Kah, L. C.; Riding, R. (2007). Mesoproterozoic carbon dioxide levels inferred from calcified cyanobacteria. **Geology**, 35(9), p. 799–802.

Kjarsgaard, B. A.; Wit, M.; Heaman, L. M.; Pearson, D. G.; Stiefenhofer, J.; Janusczcak, N.; Shirey, S. B. (2022). A Review of the Geology of Global Diamond Mines and Deposits. **Reviews in Mineralogy and Geochemistry**, 88, p. 1–118. http://dx.doi.org/10.2138/rmg.2022.88.01.

Knauer, L. G. (1990). Evolução geológica do pré-Cambriano da porção Centro-Leste da Serra do Espinhaço Meridional e metalogênese associada. Dissertação de Mestrado, Campinas, Instituto de Geociências, UNICAMP, 298p.

Knauer, L. G.; Schrank, A. (1993). A origem dos filitos hematíticos da Serra do Espinhaço Meridional, Minas Gerais. **Geonomos**, 1(1-2), p. 33-38.

Kurszlaukis, S.; Lorenz, V. (2008). Formation of "Tuffisitic Kimberlites" by phreatomagmatic processes. **Journal of Volcanology and Geothermal Research**, 174, p. 68–80.

Lai, M. Y.: Stachel, T.: Stern, R. A.: Lia, K.: Pearson, G. D.: Harris, J. W. (2023). Nature of slab-mantle interactions recorded by coupled d^{13}C–d^{15}N–d^{18}O signatures and elemental compositions of Koidu diamonds and their inclusions. **Geochimica et Cosmochimica Acta**, 347, p. 16–27.

Machado, N.; Schrank, A.; Abreu, F. R.; Knauer, L. G.; Almeida-Abreu, P. A. (1989) Resultados preliminares da geocronologia U/Pb na Serra do Espinhaço Meridional. 5º Simpósio de Geologia de Minas Gerais, Belo Horizonte, SBG, p. 171-174.

Martins-Neto, M. A. (1998). O Supergrupo Espinhaço em Minas Gerais: Registro de uma bacia Rifte-Sag do Paleo/Mesoproterozóico. **Revista Brasileira de Geociências**, 28(2), p. 151–168.

Martins-Neto, M. A. (2000). Tectonics and sedimentation in a paleo/mesoproterozoic rift-sag basin (Espinhaço basin, southeastern Brazil). **Precambrian Research**, 103, p. 147–173.

Mazumder, R.; De, S.; Sunder Raju, P.V. (2019). Archean-Paleoproterozoic transition: The Indian perspective. **Earth-Science Reviews**, 188, p. 427–440. https://doi.org/10.1016/j.earscirev.2018.11.013.

Mazumder, R.; Chaudhuri, T.; De, S.; Bauer, W.; Al Hadi, M.; Sugitani, K.; van Zuilen, M. A.; Senda, R.; Yamamoto, M.; Raju, P.V.S.; Ohta, T.; Catuneanu, O.; Mazumder, S.; Saito, S.; Shimooka, K. (2022). Paleoarchean surface processes and volcanism: Insights from the eastern Iron Ore Group, Singhbhum craton, India. **Earth-Science Reviews**, 232(104122). https://doi.org/10.1016/j.earscirev.2022.104122.

Medaris Jr., L. G.; Singer, B. S.; Jicha, B. R.; Malone, D. H.; Schwartz, J. J.; Stewart, E. K.; Lankvelt, A. van; Williams, M. L.; Reiners, P. W. (2021). Early Mesoproterozoic evolution of midcontinental Laurentia: Defining the geon 14 Baraboo orogeny. **Geoscience Frontiers**, 12(5), p. 101174.

Miranda, R. F. (2109). Caracterização geológica das metabrechas quartzíticas da Formação Sopa Brumadinho- MG: Um estudo de caso das lavras Brumadinho e Córrego Novo. Dissertação de Mestrado, PPGGeo-ICT, Universidade Federal dos Vales do Jequitinhonha e Mucuri, 77 pp.

Mitchell, R. H.; Brunfelt, A. O. (1975). Rare Earth element geochemistry of kimberlite. **Physics and chemistry of the Earth**. 9, p. 671-686.

Mitchel, R. H.; Bergman, S. C. (1991). Petrology of Lamproites. **Springer Science**, 37, p. 327 – 330.

Moraes, L. J.; Guimarães, D. (1929). Estudos sobre a rocha matriz do diamante. DNPM - SGM, **Relatório Anual Diretoria**, 1928, p. 171 - 174.

Pflug, R. (1965). A geologia da parte meridional da Serra do Espinhaço e zonas adjacentes, Minas Gerais. DNPM/DGM, **Boletim 226**.

Pflug, R. (1968). Observações sobre a estratigrafia da Série Minas na região de Diamantina, Minas Gerais. DNPM/DGM, **Notas Preliminares de Estudos 142**, 20 p.

Pflug, R.; Renger, F. E. (1973). Estratigrafia e evolução geológica da margem do Craton Sanfranciscano. 27° Congresso Brasileiro de Geologia, SBG, 2, p. 5 – 19.

Pintér, Z.; Foley, S. F.; Yaxley, G. M. (2022). Diamonds, dunites, and metasomatic rocks formed by melt/rock reaction in craton roots. **Communications Earth and Environment**, 3(1), p. 296.

Pittari, A.; Cas, R. A. F.; Lefebvre, N.; Robey, J.; Kurszlaukis, S.; Webb, K. (2008). Eruption processes and facies architecture of the Orion Central kimberlite volcanic complex, Fort à la Corne, Saskatchewan; kimberlite mass flow deposits in a sedimentary basin. **Journal of Volcanology and Geothermal Research**, 174, p. 152–170.

Porrit, L. A.; Cas, R. A. F.; Crawford, B. B. (2008). In-vent column collapse as an alternative model for massive volcaniclastic kimberlite emplacement: An example from the Fox kimberlite, Ekati Diamond Mine, NWT, Canada**. Journal of Volcanology and Geothermal Research**, 174, p. 90-102.

Regier, M. E.; Smit, K. V.; Chalk, T. B.; Stachel, T.; Stern, R. A.; Smith, E. M.; Foster, G. L.; Bussweiler, W.; DeBuhr, C.; Burnham, A. D.; Harris, J. W.; Pearson, D. G. (2023). Boron isotopes in blue diamond record seawater-derived fluids in the lower mantle. **Earth and Planetary Science Letters**, 602, p. 117923.

Renger, F. E.; Knauer, L. G. (1995). Espinhaço quo vadis? (Onde está? Aonde vai?) A evolução dos conhecimentos sobre a cordilheira do Espinhaço meridional em Minas Gerais entre 1979 e 1995. **Geonomos**, 3(1), p. 31-39.

Renger, F. E.; Almeida-Abreu, P. A.; Neves, S. C.; Fraga, L. M. S. (2025). Dados da produção e da ocorrência de grandes diamantes da província diamantífera da Serra do Espinhaço Meridional, Minas Gerais, Brasil: registro histórico e da memória oral e sua significância geológica. Geologia-USP, **Série Científica**, 25(3), p. 103–13. https://doi.org/10.11606 /issn.2316-9095.v.25-225869

Retallack, G. J.; Schmitz, M. D. (2023). Archean (3.3 Ga) paleosols and paleoenvironments of Western Australia. **PLoS ONE**, 18(9), p. 0291074. https://doi.org/10.1371/journal.pone.0291074

Rolim, V. K.; Rosière, C. A.; Santos, J. O. S.; McNaughton, N. J. (2016). The Orosirian Statherian banded iron formation-bearing sequences of the southern border of the Espinhaço Range, Southeast Brazil. **Journal of South American Earth Science**, 65, p. 43–66.

Santos, M. N.; Chemale Jr., F.; Dussin, I. A.; Martins, M. S.; Assis, T. A. R.; Jelinek, A. R.; Guadagnin, F.; Armstrong, R. (2013). Sedimentological and paleoenvironmental constraints of the Statherian and Stenian Espinhaço Rift System, Brazil. **Sedimentary Geology**, 290, p. 47–59.

Schöll, W. U.; Fogaça, A. C. C. (1979). Estratigrafia da Serra do Espinhaço na região de Diamantina. 1º Simpósio de Geologia de Minas Gerais, Diamantina, SBG, **Boletim 1**, p. 55–73.

Sheldon, N. D.; Mitchell, R. L.; Dzombak, R. M. (2021). Reconstructing Precambrian pCO_2 and pO_2 Using Paleosols Elements in Geochemical Tracers in Earth System Science
In: Elements in Geochemical Tracers in Earth System Science (Timothy Lyons, ed.), **Cambridge University Press**. https://doi.org/10.1017/9781108870962.

Silveira-Braga, F. C.; Rosière, C. A.; Queiroga, G. N.; Rolim, V. K.; Santos, J. O. S.; McNaughton, N. J. (2015). The Statherian itabirite-bearing sequence from the Morro Escuro Ridge, Santa Maria de Itabira, Minas Gerais, Brazil. **Journal of South American Earth Sciences**, 58, p. 33-53.

Smit, K. V.; Timmerman, S.; Aulbach, S.; Shirey, S. B.; Richardson, S. H.; Phillips, D.; Pearson, D. G. (2022). Geochronology of Diamonds. Reviews in **Mineralogy and Geochemistry**, 88, p. 567-636.

Stachel, T.; Harris, J. W. (2008). The origin of cratonic diamonds - Constraints from mineral inclusions. **Ore Geology Reviews**, 34, p. 5-32. https://doi.org/10.1016/j.oregeorev. 2007.05.002.

Sun, S. S.; McDonough, W. F. (1989). Chemical and Isotopic Systematics of Oceanic Basalts: Implications for Mantle Composition and Processes. In: Saunders, A.D., Norry, M.J., Eds., **Magmatism in the Ocean Basins**, Geological Society, London, Special Publications, 42, p. 313-345. https://doi.org/10.1144/GSL.SP.1989.042.01.19

Thompson, L. (1928). Upland diamond deposits, Diamantina District, Minas Geraes, Brazil. **Economic Geology**, XXIII, 7, p. 705-723.

ISSN 2317-0611

Timmerman, S.; Reimink, J. R.; Vezinet, A.; Nestola, F.; Kublik, K.; Banas, A.; Stachel, T.; Stern, R. A.; Luo, Y.; Sarkar, C.; Ielpi, A.; Currie, C. A.; Mircea, C.; Jackson, V.; Pearson, D. G. (2022). Mesoarchean diamonds formed in thickened lithosphere, caused by slab-stacking. **Earth and Planetary Science Letters**, 592. https://doi.org/10.1016/j.epsl.2022.117633

Tovey, M.; Giuliani, A.; Phillips, D.; Moss, S. (2020). Controls on the explosive emplacement of diamondiferous kimberlites: New insights from hypabyssal and pyroclastic units in the Diavik mine, Canada. **Lithos**, 105410, p. 360–361,.

Uhlein, A. (1991). Transição cráton-faixa dobrada: exemplo Cráton São Francisco e da Faixa Araçuaí (ciclo Brasiliano) no Estado de Minas Gerais. Aspectos estratigráficos e estruturais. Tese de doutorado, São Paulo, IG - USP, 295p.

Uhlein, A.; Trompette, R. R.; Egydio-Silva, M. (1998). Proterozoic rifting and closure, SE border of the São Francisco Craton, Brazil. **Journal of South American Earth Sciences**, 11, p. 191–203.

Walter, M. J.; Thomson, A. R.; Smith, E. M. (2022). Geochemistry of Silicate and Oxide Inclusions in Sublithospheric Diamonds. **Reviews Mineralogy Geochemistry**, 88, p. 393-450. http://dx.doi.org/10.2138/rmg.2022.88.07

Zhang, Q.; Timmerman, S.; Stachel, T.; Chinn, I.; Stern, R. A.; Davies, J.; Nestola, F.; Luth, R.; Pearson, D. G. (2024). Sublithospheric diamonds extend Paleoproterozoic record of cold deep subduction into the lower mantle. **Earth and Planetary Science Letters**, 634. https://doi.org/10.1016/j.epsl.2024.118675